Preprints (www.preprints.org) | NOT PEER-REVIEWED | Posted: 11 September 2020 doi:10.20944/preprints202009.0141.v2

Nonlinear approximations to critical and relaxation processes

Simon Gluzman
Materialica + Research Group, Bathurst St. 3000, Apt. 606, Ontario M6B 3B4, Toronto, Canada (simongluzmannew@gmail.com)

Abstract

We discuss methods for calculation of critical indices and amplitudes from the perturbative expansions. Several important examples of the Stokes flow through 2D and 3D channels are brought up. Power series for the permeability derived for small values of amplitude are employed to calculation of various critical exponents in the regime of large amplitudes. Special nonlinear approximations valid for arbitrary values of the wave amplitude are derived from the expansions.

The technique developed for critical phenomena is applied then for relaxation phenomena. The concept of time-translation invariance is discussed, its spontaneous violation and restoration considered. Emerging probabilistic patterns correspond to a local breakdown of time-translation invariance. Their evolution leads to the time-translation symmetry complete (or partial) restoration. We estimate typical time extent, amplitude and direction for such restorative process. The new technique is based on explicit introduction of origin in time. After some transformations we come to the exponential and generalized, exponential-type solution with explicit finite time scale, which was only implicit in initial parametrization with polynomial approximation. The concept of crash as a relaxation phenomenon, consisting of time-translation invariance breaking and restoration, is put forward. COVID-19 related mini-crash in the time series for Shanghai Composite is discussed as an illustration.

1 Introduction

Let the function $\Phi(x)$ of a real variable $x \in [0, \infty)$ be defined by some complicated problem. Such problem does not allow for an explicit solution

© 2020 by the author(s). Distributed under a Creative Commons CC BY license.

Preprints (www.preprints.org) | NOT PEER-REVIEWED | Posted: 11 September 2020 doi:10.20944/preprints202009.0141.v2

to the function form. The variable $x > 0$ can represent, e.g., a coupling constant or concentration. And let as assume some kind of perturbation theory is possible to develop, so that it generates asymptotic expansions about the point $x = x_0 = 0$,

$$\Phi(x) \sim \sum_{n=0}^{\infty} c_n x^n. \tag{1}$$

Our task is to recast the divergent series into convergent expressions by means of analytical constructs, the so-called approximants.

One can always extrapolate the perturbative results by means of the Padé approximants $P_{n,m}(x)$ [1]. Unfortunately, solutions to many problems exhibit irrational functional behavior. It cannot be properly described by Padé approximants. Sometimes they are are not applicable at all. But it would be highly desirable to modify somehow the familiar technique of Padé approximants. Such modification can be performed by separating the sought replacement into two factors [2]. One factor is to be expressed as iterated root approximant or factor approximant [3, 9], is particularly designed to take care of the irrational part of the solution. The other factor is simply a Padé approximant, is supposed to take care of the rational part of the solution. We arrive thus to the corrected Padé approximants. They appear to be applicable to a larger class of problems, even when the standard Padé technique is not applicable [3]. Many more applications of the Padé approximants and their modifications could be found in [4].

The Padé approximants $P_{M,N}$ can be understood simply as ratio of the two polynomials $P_M(x)$ and $Q_N(x)$ of the order M and N, respectively. The diagonal Padé approximant of order N corresponds to the case of $M = N$. Conventionally, $Q_N(0) = 1$. The coefficients of the polynomials are derived directly from the asymptotic equivalence with the given power series for the sought function $\Phi(x)$. The notation for Padé approximants used in the paper is conventional. Sometimes, when there is a need to stress the role of $\Phi(x)$, we are going to write $PadeApproximant\,[\Phi[x], n, m]$.

A Padé approximant might posses a pole associated with a finite critical point, but can only produce an integer critical index. While usually critical indices are not integers. The same concerns the large-variable behavior where the power of x produced from extrapolation with some form of Padé approximants is always an integer. Two-point Padé are applied for interpolation, when in addition to the expansion about $x_0 = 0$, given by (1), an additional information is available and contained in the expansion about $x = \infty$.

Preprints (www.preprints.org) | NOT PEER-REVIEWED | Posted: 11 September 2020 doi:10.20944/preprints202009.0141.v2

There are four main technical approaches to constructing approximants with the goal to optimize their performance. The first approach is conventional, also called accuracy-through order, and is based on progressive improvement of quality with adding new information with the approximants becoming more and more complex. It is exemplified in construction of Pad'e and Euler super-exponential approximants, factor, root and additive approximants [3].

Second approach leads to corrected approximants. The idea is to ensure the correct form of the solution already in the starting approximation with some initial parameters. The initial parameters should be corrected by asymptotically matching with the truncated series/regressions in increasing orders. So, instead of increasing the order of approximation, one can correct the parameters of the initial approximation [3, 9]. So, the form of the solution is not getting more complex, but the parameters take more and more complex form with increasing order. Corrected approximants will complement the third approach, when there are no solutions within the framework of the third approach.

In the third approach predominantly adopted in Section 4, we keep the form and order of approximants the same in all orders, but let the series/regressions evolve into higher orders. Independent on the order of regression, we construct the same approximant, based only on the first order terms, only with parameters changing with increasing order of regression. In the framework of effective first order theories, we employ exponential approximants.

In the fourth approach the critical index is treated as vital part of optimization procedure. It plays the role of a control parameter, sometimes even of a control function, to be determined from optimization procedure described in the Section 2.2, following [50]. Some other optimization techniques based on introduction of an additional control parameters, were proposed in [51, 52].

2 Critical index and relaxation time

We are going to speak about the critical behavior with a critical index α, at a finite critical point x_c, when

$$\Phi(x) \simeq A(x_c - x)^{\alpha}, \text{ as } x \to x_c - 0 \, . \tag{2}$$

Preprints (www.preprints.org) | NOT PEER-REVIEWED | Posted: 11 September 2020 doi:10.20944/preprints202009.0141.v2

The definition covers the case of negative index when function can tend to infinity, or the sought function can tend to zero if the index is positive. Sometimes, the values of critical index and critical point are known from some sources, and the problem consists in finding the critical amplitude A, as extensively exemplified in [3].

The case when critical behavior occur at infinity,

$$\Phi(x) \simeq Ax^{\alpha}, \text{ as } x \to \infty \, , \tag{3}$$

can be analyzed similarly. It can be understood as the particular case with the critical point positioned at infinity.

Critical phenomena are ubiquitous [50], ranging from the field theory to hydrodynamics. And it is vital to explain related critical indices theoretically. Regrettably, for realistic physical systems one can as a rule learn only its behavior at small variable,

$$\Phi(x) \simeq \Phi_k(x), \text{ as } x \to 0 \, . \tag{4}$$

Thus the function is approximated by an expansion

$$\Phi_k(x) = 1 + \sum_{n=1}^{k} c_n x^n \, . \tag{5}$$

Such expansions are usually asymptotic. They strongly diverge and their use is permitted only at some small values of the variable.

The critical exponents can be found by using definition of the critical index. One can express the critical index directly, and find it as the limit of explicitly expressed approximants. For instance, critical index can be estimated from a standard representation as following derivative

$$\mathcal{B}_a(x) = \partial_x \log(\Phi(x)) \simeq \frac{-\alpha}{x_c - x}, \tag{6}$$

as $x \to x_c$, thus defining critical index as the residue in the corresponding single pole. The pole corresponds to the critical point x_c. The critical index corresponds to the residue

$$\alpha = \lim_{x \to x_c} (x - x_c)\mathcal{B}_a(x).$$

To the *DLog*-transformed series one is bound to apply the Padé approximation. Moreover, the whole table of Padé approximants can be constructed

Preprints (www.preprints.org) | NOT PEER-REVIEWED | Posted: 11 September 2020 doi:10.20944/preprints202009.0141.v2

[1]. I.e. the *DLog* Padé method does not lead to a unique algorithm for finding critical indices. procedure. Basically different values are produced by different Padé approximants. Then it is not clear which of these quantities to prefer. Standard approach consists in applying a diagonal Padé approximants.

When a function, at asymptotically large variable, behaves as in (3), then the critical exponent can be defined similarly, by means of the *DLog* transformation. It is represented by the limit

$$\alpha = \lim_{x\to\infty} x\mathcal{B}_a(x) \ . \tag{7}$$

Assume that the small-variable expansion for the function $B_a(x)$ is given. In order that the critical index be finite it is necessary to take the asymptotically equivalent approximants behaving as x^{-1} as $x \to \infty$. It leaves us no choice but to select the non-diagonal Padé $P_{n,n+1}(x)$ approximants, so that the corresponding approximation α_n is finite. One can also apply, in place of Padé, some different approximants. To this end one should apply the transformation,

$$z = \frac{x}{x_c - x} \ \Leftrightarrow \ x = \frac{zx_c}{z+1} \tag{8}$$

to the original series and reduce the problem of finding critical index to the previous case.

To simplify and standardize calculations different, and more powerful approximants, called self-similar factor approximants have been introduced in Refs. [6]. The k-th order self-similar factor approximant reads as

$$\mathcal{F}_k^*(x) = c_0 \prod_{i=1}^{N_k} (1 + \mathcal{P}_i x)^{m_i} \ , \tag{9}$$

where

$$N_k = \tfrac{k}{2}, \quad k = 2, 4, \ldots; \quad N_k = \tfrac{k+1}{2}, \quad k = 3, 5, \ldots \tag{10}$$

and the parameters $\mathcal{P}_i$ and m_i are defined typically from the asymptotic equivalence complemented with additional constraints on the sought function. For even order, the above procedure uniquely defines all $k = 2p$ parameters. In odd case $k = 2p + 1$, one is obliged to impose some extra condition motivated by the problem, and uniquely defining all other parameters. The singular solutions emerging from factor approximants correspond to critical points and phase transitions [6], including also the case of singularity located

Preprints (www.preprints.org) | NOT PEER-REVIEWED | Posted: 11 September 2020 doi:10.20944/preprints202009.0141.v2

at ∞. It is very difficult to improve factor approximants when the series are short, unless some additional asymptotic (or point-wise) information on the critical point is available. Some suggestions on such improvement were advanced on [9]. When the series are long one would expect that the accuracy is going to improve with increasing number of terms. Sometimes, an optimum is achieved for some finite number of terms. reflecting on the asymptotic nature of the underlying series.

2.1 Relaxation time

Consider the case of relaxation behavior when a function at asymptotically large variable decays as

$$\Phi(t) \simeq A \exp(\frac{t}{\tau}) \qquad (t \to \infty) \; , \tag{11}$$

with negative τ. Formally, the relaxation time is $-\tau$. It can be found as the limit

$$\frac{1}{\tau} = \lim_{t\to\infty} \frac{d}{dt} \; \ln \Phi(t) \; . \tag{12}$$

Just as in the case of critical behavior considered above, the small-variable expansion for the function is given by the sum $\Phi_k(t)$. The effective relaxation time can be expressed in terms of the small-variable expansion as follows,

$$\frac{1}{\tau_k(t)} = \frac{d}{dt} \; \ln \Phi_k(t) \; . \tag{13}$$

It can be expanded in powers of t, leading to

$$\tau_k(t) = \sum_{n=0}^{k} b_n t^n \; . \tag{14}$$

The coefficients b_n are easily expressed through c_n of the original series (1). Let us apply to the obtained expansion the self-similar or Padé approximants. I.e., we have to derive an approximant $\tau_k^*(t)$ whose limit

$$\tau_k^*(t) \to const \qquad (t \to \infty) \; ,$$

gives the relaxation time

$$\tau_k^* = \lim_{t\to\infty} \tau_k^*(t) \; . \tag{15}$$

Preprints (www.preprints.org) | NOT PEER-REVIEWED | Posted: 11 September 2020 doi:10.20944/preprints202009.0141.v2

In such approach the amplitude A does not enter the consideration. In practice one can indeed construct the approximants with such required behavior. The complete approximant for the sought function $\Phi(t)$ denoted below as $E(t,r)$, can be constructed as well. Even some *ad hoc* forms satisfying some general symmetry requirements can be suggested, as in the Section 4.

As an illustration, let us find $\tau_k^*(t)$ in explicit form under some simple assumptions concerning its asymptotic behaviors. Assume simply that there are two distinct exponential behaviors for short and long times with two different τ_1, τ_2, and the transition from short to long time behavior also occur at the duration of some third characteristic time $\tau_3 = -\beta_3^{-1}$. The characteristic times can be found from the short-time expansion. The simple approximation to the effective relaxation time expressed in second order of (15), can be written down in the spirit of [7] as follows,

$$\tau_2{}^*(t)^{-1} = \beta_2 + (\beta_1 - \beta_2)\exp(\beta_3 t), \tag{16}$$

so that for negative β_3 we have $\tau_2^*(0)^{-1} = \beta_1$, $\tau_2^*(\infty)^{-1} = \beta_2$. In the theory of reliability the failure(hazard) rate or mortality force [8], are analogous to the inverse effective relaxation time, and the model of the type of formula (16) is known as Gompertz-Makeham law of mortality.

The complete approximant corresponding to (16) is reconstructed after elementary integration

$$F(t) = A\exp\left(\frac{(\beta_1 - \beta_2)\exp(\beta_3 t)}{\beta_3} + \beta_2 t\right), \tag{17}$$

with all unknown constituents of (16) expressed explictly, from the asymptotic equivalence with the power-series,

$$A = c_0\exp\left(\frac{\left({c_1}^2 - 2c_0c_2\right)^3}{4(3{c_0}^2c_3 - 3c_0c_1c_2 + {c_1}^3)^2}\right), \quad \beta_1 = \frac{c_1}{c_0}, \quad \beta_2 = \frac{6{c_0}^2c_1c_3 - 4{c_0}^2{c_2}^2 - 2c_0{c_1}^2c_2 + {c_1}^4}{2c_0(3{c_0}^2c_3 - 3c_0c_1c_2 + {c_1}^3)},$$
$$\beta_3 = \frac{2\left(3{c_0}^2c_3 - 3c_0c_1c_2 + {c_1}^3\right)}{c_0(2c_0c_2 - {c_1}^2)}. \tag{18}$$

Most interesting, as $\beta_2 = 0$, we arrive in different notations to the Gompertz function (99),

$$G(t) = A\exp\left(\frac{\beta_1\exp(\beta_3 t)}{\beta_3}t\right), \tag{19}$$

employed in calculations of [28]. In this case we have the effective relaxation time decaying exponentially with time. In the Section 4 we apply this method of finding the effective relaxation time for time series.

Preprints (www.preprints.org) | NOT PEER-REVIEWED | Posted: 11 September 2020 doi:10.20944/preprints202009.0141.v2

2.2 Critical index as control parameter. Optimization technique

The function's critical behavior follows from extrapolating the asymptotic expansion (1) to finite or large values of the variable. Such an extrapolation can be accomplished by means of a direct techniques just discussed above. But their successful application requires knowledge of a large number of terms in the expansion. But it is also possible to obtain rather good estimates for the critical indices from a small number of terms in the asymptotic expansion [50]. To this end we can employ the self-similar root approximants given by (20). The external power m_k is to be determined here from additional conditions.

The self-similar root approximant has the following general form

$$\mathcal{R}_k^*(x, m_k) = \left(\left((1 + \mathcal{P}_1 x)^{m_1} + \mathcal{P}_2 x^2 \right)^{m_2} + \ldots + \mathcal{P}_k x^k \right)^{m_k} . \tag{20}$$

In principle, all the parameters may be found from asymptotic equivalence with given power series.

The large-variable power α in equation (3) could be compared with the large-variable behavior of the root approximant (20),

$$\mathcal{R}_k^*(x, m_k) \simeq A_k x^{k m_k} , \tag{21}$$

where

$$A_k = \left(\left(\mathcal{P}_1^{m_1} + \mathcal{P}_2 \right)^{m_2} + \mathcal{P}_3 \right)^{m_3} + \ldots + \mathcal{P}_k \Big)^{m_k} . \tag{22}$$

This comparison yields the relation $k m_k = \alpha$, defining the external power $m_k = \frac{\alpha}{k}$, when α is known. This way of defining the external power is used when the root approximants are applied for interpolation.

Consider an exceptionally difficult situation: the large-variable behavior of the function is not known and α is not given. In addition, the critical behavior can happen at a finite value x_c of the variable x. The method for calculating the critical index α by employing the self-similar root approximants was developed in [50].

In such approach we construct several root approximants $R_k^*(x, m_k)$, and the external power m_k plays the role of a control function. The sequence of approximants is considered as a trajectory of a dynamical system. The approximation order k plays the role of discrete time. A discrete-time dynamical system or the approximation cascade, consists of the sequence of

Preprints (www.preprints.org) | NOT PEER-REVIEWED | Posted: 11 September 2020 doi:10.20944/preprints202009.0141.v2

approximants. The cascade velocity is defined by Euler discretization formula [53, 54, 55]

$$V_k(x, m_k) = \mathcal{R}^*_{k+1}(x, m_k) - \mathcal{R}^*_k(x, m_k) + (m_{k+1} - m_k) \frac{\partial}{\partial m_k} \mathcal{R}^*_k(x, m_k) \ . \quad (23)$$

The effective limit of the sequence of approximants corresponds to the fixed point of the cascade. Based on just a few approximants, the cascade velocity has to decrease. In such sense the sequence appears to be convergent. And the control functions $m_k = m_k(x)$, have to minimize the absolute value of the cascade velocity

$$|V_k(x, m_k(x))| = \min_{m_k} |V_k(x, m_k)| \ . \quad (24)$$

A finite critical point x^c_k, in the k-th approximation, is to be obtained from the equation

$$[\mathcal{R}^*_k(x^c_k, m_k)]^{1/m_k} = 0 \qquad (0 < x^c_k < \infty). \quad (25)$$

Its finite solution is denoted as $x^c_k = x^c_k(m_k)$.

The critical index in the k-th approximation is given by the limit

$$\alpha_k = \lim_{x \to x^c_k} m_k(x).$$

In the case of the critical behavior at infinity, when as $x_c \sim \infty$, the critical index is

$$\alpha = k \lim_{x \to \infty} m_k(x), \ as \ x_c \sim \infty \ . \quad (26)$$

Thus, to find the critical indices, the control functions $m_k(x)$ have to be found. The minimization of the cascade velocity (96) is complicated. The equation (24) contains two control functions, m_{k+1} and m_k. Nevertheless the problem can be resolved.

The first constructive approach notices that m_{k+1} should be close to m_k. Then we arrive to to the *minimal difference condition*

$$\min_{m_k} \left| \mathcal{R}^*_{k+1}(x, m_k) - \mathcal{R}^*_k(x, m_k) \right| \qquad (k = 1, 2, \ldots) \ . \quad (27)$$

One should typically find a solution $m_k = m_k(x)$ of the simpler equation

$$\mathcal{R}^*_{k+1}(x, m_k) - \mathcal{R}^*_k(x, m_k) = 0 \ . \quad (28)$$

Preprints (www.preprints.org) | NOT PEER-REVIEWED | Posted: 11 September 2020 doi:10.20944/preprints202009.0141.v2

The control functions m_k, characterizing the critical behavior of $\Phi(x)$ become the numbers $m_k(x_c)$. We simply write $m_k = m_k(x_c)$.

In the vicinity of a finite critical point, the function $\mathcal{R}_k^*$ behaves as

$$\mathcal{R}_k^*(x, m_k) \simeq \left(1 - \frac{x}{x_k^c}\right)^{m_k}, \ as \ x \to x_k^c - 0 \ . \tag{29}$$

The condition (28)is expressed as follows,

$$x_{k+1}^c(m_k) - x_k^c(m_k) = 0 \qquad (0 < x_k^c < \infty) \ . \tag{30}$$

For the critical behavior at infinity, it is expedient to introduce the control function

$$\mathsf{s}_k = k m_k \ . \tag{31}$$

And the large-variable behavior reads as

$$\mathcal{R}_k^*(x, \mathsf{s}_k) \simeq A_k(\mathsf{s}_k) x^{\mathsf{s}_k}, \ as \ x \to \infty \ . \tag{32}$$

As a result, the minimal difference condition is reduced to the equation

$$A_{k+1}(\mathsf{s}_k) - A_k(\mathsf{s}_k) = 0, \ as \ x_k^c \sim \infty \ . \tag{33}$$

The alternative equation for the control functions also follows from the minimal velocity condition (24), and is called the minimal derivative condition

$$\min_k \left| \frac{\partial}{\partial m_k} \mathcal{R}_k^*(x, m_k) \right| \qquad (k = 1, 2, \ldots) \ , \tag{34}$$

In practice we have to solve the equation

$$\frac{\partial}{\partial m_k} \mathcal{R}_k^*(x, m_k) = 0 \ . \tag{35}$$

To apply this condition, we have first to extract from the function its non-divergent parts. If the critical point is finite, one can study the residue of the function $\partial \log \mathcal{R}_k^* / \partial m_k$, expressed as

$$\lim_{x \to x_k^c} (x_k^c - x) \frac{\partial}{\partial m_k} \log \mathcal{R}_k^*(x, m_k) = m_k \frac{\partial x_k^c}{\partial m_k} \ .$$

Thus, from equation (35), we arrive to the condition

$$\frac{\partial x_k^c}{\partial m_k} = 0 \qquad (0 < x_k^c < \infty) \ . \tag{36}$$

Preprints (www.preprints.org) | NOT PEER-REVIEWED | Posted: 11 September 2020 doi:10.20944/preprints202009.0141.v2

When the critical behavior occurs at infinity, then we can consider the limiting form of the amplitude and reduce the equation (35) to the form

$$\frac{\partial A_k(\mathsf{s}_k)}{\partial \mathsf{s}_k} = 0, \ as \ x_k^c \sim \infty \ . \tag{37}$$

Let us consider as example the case of the two-dimensional channel bounded by the surfaces $z = \pm b \, (1 + \epsilon \cos x)$. Here ϵ is termed *waviness*. The permeability behaves critically [11]. I.e., it tends to zero as

$$K(\epsilon) \sim (\epsilon_c - \epsilon)^{\varkappa}, \ \text{as} \ \epsilon \to \epsilon_c - 0 \ , \tag{38}$$

with $\epsilon_c = 1$, $\varkappa = \frac{5}{2}$. The permeability as a function of the waviness can be derived in the form of an expansion in powers of ϵ [11, 13]. In the particular case of $b = 0.5$, the permeability can be found explicitly as

$$K(\epsilon) \simeq 1 - 3.14963 \, \epsilon^2 + 4.08109 \, \epsilon^4, \ \text{as} \ \epsilon \to 0 \ . \tag{39}$$

By setting $\epsilon_c = 1$, and changing the variable $y = \frac{\epsilon^2}{1-\epsilon^2}$, one can move the critical point to infinity. The critical index is calculated as explained above and in [50]. From the minimal-difference condition we find $\varkappa_1 = 2.184$, with an error 12.6%. From the minimal derivative condition we obtain $\varkappa_2 = 2.559$, with an error 2.37%. The final answer $\varkappa^*$ is given by the average of two solutions $\varkappa^* = 2.372 \pm 0.19$.

In another particular case, for $b = 0.25$, the permeability expands as follows,

$$K(\epsilon) \simeq 1 - 3.03748 \, \epsilon^2 + 3.54570 \, \epsilon^4, \ \text{as} \ \epsilon \to 0 \ . \tag{40}$$

Setting $\epsilon = 1$, and using the same technique as above the approximations for critical index are found, so that $\varkappa_1 = 2.342$, and $\varkappa_2 = 2.743$. Finally, $\varkappa^* = 2.543 \pm 0.2$.

Let us also consider some examples of the numerical convergence of root approximants in high-orders. The technique is applied again for calculating critical index $\varkappa$. It seems instructive to consider the same two cases of permeability $K(\epsilon)$, but with higher-order terms, up to 16th order inclusively.

The numerical form of the corresponding expansions can be found in Section 3, see expansion (56), and expansion (65). Concretely, we construct the iterated root approximants

$$\mathcal{R}_k^*(y) = \left(\left(\left((1 + \mathcal{P}_1 y)^2 + \mathcal{P}_2 y^2 \right)^{3/2} + \mathcal{P}_3 y^3 \right)^{4/3} + \ldots + \mathcal{P}_k y^k \right)^{\alpha/k} . \tag{41}$$

Preprints (www.preprints.org) | NOT PEER-REVIEWED | Posted: 11 September 2020 doi:10.20944/preprints202009.0141.v2

The parameters $\mathcal{P}_j$ have to be found from the asymptotic equivalence with the expansions. The permeability has the required critical asymptotic forms

$$\mathcal{R}_k^*(y) \simeq A_k y^{\alpha}, \ as \ y \to \infty \ . \tag{42}$$

And the amplitudes $A_k = A_k(\alpha_k)$ are found explicitly as

$$A_k = \Big(\big((\mathcal{P}_1^2 + \mathcal{P}_2)^{3/2} + \mathcal{P}_3 \big)^{4/3} + \ldots + \mathcal{P}_k \Big)^{\alpha/k} \ . \tag{43}$$

To define the critical index α_k, we analyze the differences

$$\Delta_{kn}(\alpha_k) = A_k(\alpha_k) - A_n(\alpha_k) \ . \tag{44}$$

From the sequences $\Delta_{kn} = 0$, we find the related sequences of approximate values α_k for the critical indices.

Although it is possible to investigate different sequences of the conditions $\Delta_{kn} = 0$, the most natural from is presented by the sequences of $\Delta_{k,k+1} = 0$ and of $\Delta_{k8} = 0$, with $k = 1, 2, 3, 4, 5, 6, 7$.

The results for $b = \frac{1}{2}$, are shown in Table 1. We observe good numerical convergence of the approximations $\alpha_k \equiv \varkappa_k$, to the value $\varkappa = \frac{5}{2}$.

Similar results, presented in Table 2 (for $b = \frac{1}{4}$), again demonstrate rather good numerical convergence of the approximate critical indices to the value $\varkappa = \frac{5}{2}$.

The critical index does not depend on parameter b. The *DLog* Padé method appears to bring convergent sequences and consistent expressions for permeability as well. Further details to be found in the Section 3.

Consider yet different case of permeability $K(\epsilon)$, see Section 3, subsection 3.1.3. For the parallel sinusoidal two-dimensional channel the walls would not touch. The permeability remains finite. It is expected to decay as a power-law as ϵ becomes large,

$$K(\epsilon) \sim \epsilon^{\nu}, \ \text{as} \ \epsilon \to \infty,$$

with negative index ν.

In the expansion of $K(\epsilon)$ in small parameter ϵ^2 we retain the same number of terms as in previous two examples. The numerical values of the corresponding coefficients can be found in Section 3, see expansion (68) on page 24. Results of calculations are presented in Table 3 (for $b = \frac{1}{2}$), and show good numerical convergence, especially in the last column, to the value -4. The sequence, based on the *DLog* Padé method, is convergent as well, see Section 3, subsection 3.1.3.

Preprints (www.preprints.org) | NOT PEER-REVIEWED | Posted: 11 September 2020 doi:10.20944/preprints202009.0141.v2

$\varkappa_k$	$\Delta_{k+1}(\varkappa_k)=0$	$\Delta_{k8}(\varkappa_k)=0$
$\varkappa_1$	2.18445	2.39678
$\varkappa_2$	2.68311	2.52028
$\varkappa_3$	2.48138	2.49208
$\varkappa_4$	2.49096	2.49692
$\varkappa_5$	2.5012	2.49982
$\varkappa_6$	2.49935	2.499
$\varkappa_7$	2.49861	2.49861

Table 1: Wall can touch (b=1/2). Critical indices for the permeability $\varkappa_k$ obtained from the optimization found from the optimization conditions (44). There is rather good numerical convergence to the theoretical number $\varkappa = 5/2$.

$\varkappa_k$	$\Delta_{k+1}(\varkappa_k)=0$	$\Delta_{k8}(\varkappa_k)=0$
$\varkappa_1$	2.34165	2.452
$\varkappa_2$	2.52463	2.50542
$\varkappa_3$	2.4976	2.49933
$\varkappa_4$	2.49941	2.50004
$\varkappa_5$	2.50028	2.50033
$\varkappa_6$	2.50032	2.50036
$\varkappa_7$	2.50041	2.50041

Table 2: Walls can touch (b=1/4). Critical indices $\varkappa_k$ found from the optimization conditions (44). There is a good numerical convergence of the sequences to the theoretical value $\varkappa = 5/2$.

Preprints (www.preprints.org) | NOT PEER-REVIEWED | Posted: 11 September 2020 doi:10.20944/preprints202009.0141.v2

ν_k	$\Delta_{k+1}(\nu_k)=0$	$\Delta_{k8}(\nu_k)=0$
ν_1	-6	-4.36
ν_2	-4.04	-4.1
ν_3	n.a.	-4.13
ν_4	-4.09	-4.05
ν_5	-3.97	-4.03
ν_6	n.a.	-4.08
ν_7	-3.94	-3.94

Table 3: Walls can not touch. Case of b=1/2. Critical indices for the permeability for the problem of Section 3, subsection 3.1.3, obtained from the optimization conditions $\Delta_{kn}(\nu_k)=0$. The sequences demonstrate reasonably good numerical convergence to the value $\nu=-4$.

3 Critical permeability

Critical behavior of permeability of certain models of Darcy flow in porous media, treatable with power-series, is studied in this section. Permeability of spatially periodic arrays of cylinders was analyzed and found in analytical form in [9]. Transverse flow past hexagonal and square arrays of cylinders was studied as well, based on expansions for small concentrations and lubrication approximation for high concentrations of cylinders [9]. 3D periodic arrays of spherical obstacles are discussed in [9] as well. Formulas for the drag force exerted by various lattices of obstacles were derived from the low-concentration expansions.

Below, the important for applications problem of Stokes flow through a 2D and 3D channels enclosed by two wavy walls is studied. It is considered by means of the approach combining analytical and numerical approach to derivation of expansions and approximants. Compact formulas for the permeability are derived in the form of approximants for all required values of amplitude. Various power-laws are found by extrapolation in the regime of large amplitudes, based only on expansions at small amplitudes. Despite of the popular lubrication approximation breakdown, it is still possible to obtain accurate formulas for the effective permeability for arbitrary values of the wave amplitude. In principle, only are the expansions for small amplitudes are involved. But they have to be complemented by some general knowledge on the critical point position, and about existence of the critical index for permeability.

Preprints (www.preprints.org) | NOT PEER-REVIEWED | Posted: 11 September 2020 doi:10.20944/preprints202009.0141.v2

This section deals exclusively with constructive analytical solutions. In other words with approximate analytical solutions, when the resulting formulas contain the main physical and geometrical parameters. The available truncated series are considered as polynomials. They remember their infinite expansions, so that with a help of some specially crafted resummation procedure one can extrapolate to the whole series by means of carefully derived approximants. The approximants are asymptotically equivalent to the truncated series. The approximants are more inclusive than polynomials, because they encompass various asymptotic regimes. And they generate an additional, infinite number of the coefficients in expansion.

For low Reynolds numbers R, the flow of a viscous fluid through a channel is described by the well-known Darcy's law. The Darcy law describes a linear relation between the pressure gradient $\overline{\nabla p}$ and the average velocity $\overline{u}$ along the pressure gradient [11]. It is given as follows,

$$|\overline{\nabla p}| = \frac{\eta}{K}\overline{u}, \tag{45}$$

where K stands for the permeability and η is the dynamic viscosity of the fluid. The definition of permeability simply characterizes the amount of viscous fluid flow through a porous medium per unit time and unit area when a unit macroscopic pressure gradient is applied to the system [9]. The classical Poiseuille flow is a classic example, which yields the Darcy's law. It unfolds in the channel bounded by two parallel planes separated by a distance $2b$, generated by an average pressure gradient $\overline{\nabla p}$. The flow profile is known to be parabolic when the Reynolds number R is small.

When the channel is "wavy", i.e., not straight and when the Reynolds number is not negligible, additional terms appear in this relation [13, 12]. Yet Darcy law holds in the interesting case of the Stokes flow through a channel with three-dimensional wavy walls. The enclosing wavy walls are described by the analytical expressions, including the amplitude of waviness. The amplitude is proportional to the mean clearance of the channel and is multiplied by the small dimensionless parameter ϵ.

Darcy low also is also considered for percolation models, used to model, both theoretically and experimentally, the critical behavior of the fluid permeability. A simple network of randomly distributed random pipes network serves as generic model of percolation. It is considered to be equivalent to a random resistor network. Among its various applications one subject does stand alone. The percolation model is applied to simulate fluid flow in the

Preprints (www.preprints.org) | NOT PEER-REVIEWED | Posted: 11 September 2020 doi:10.20944/preprints202009.0141.v2

case of a sea ice, vitally important for climate studies [14, 15].

The problems of permeability and conductivity belong to two different classes [10]. For small and moderate volume fractions mathematical structure of the permeability and conductivity problems is alike and Laplacian. Therefore, they both can be addressed by the same methodology. In the case of high volume fractions, such analogy does not apply. It is found that permeability and conductivity are characterized by different critical exponents [10], see also [9] for more detailed discussion of the criticality models in porous media.

An existing estimate for the fluid permeability critical exponent $\varkappa$ for sea ice, strongly suggests the value of about 2.5 [14]. We conclude here by noting that the classical hydrodynamic models to be discussed below, also demonstrate power-law behavior, around their corresponding thresholds, with the same value of the critical exponent for permeability. Thus, reality implores us to study critical phenomena directly from the hydrodynamic equations, and to calculate permeability via homogenization procedure. In the cases considered below in this section we deal with a unique theoretical opportunity to attack the problem of critical exponent and criticality in general, directly from the solution of Stokes problem, much like the problem of phase transitions is attacked directly from a concrete microscopic models [49].

3.1 Permeability in wavy-walled channels. General information

We completeness, we follow below the main steps of the derivation leading to the expansions for permeability, as obtained by Mityushev, Malevich and Adler. In Ref.[13] a general asymptotic analysis was applied to a Stokes flow in curvilinear three-dimensional channel. It is bounded by walls of rather general shape described as follows

$$z = S^{+}(x_1, x_2) \equiv b\big(1 + \epsilon T(x_1, x_2)\big), \tag{46}$$

$$z = S^{-}(x_1, x_2) \equiv -b\big(1 + \epsilon B(x_1, x_2)\big). \tag{47}$$

In what follows, the formally small dimensionless parameter $\epsilon \geq 0$ is considered. It is introduced in such a way to allow the general form (46), to be recast as the geometric perturbation. The expansion is accomplished around the straight channel considered as zero-approximation.

Preprints (www.preprints.org) | NOT PEER-REVIEWED | Posted: 11 September 2020 doi:10.20944/preprints202009.0141.v2

Such approach builds on an original work by Pozrikidis [17], on two-dimensional case. This approach could be extended to the gravity driven Stokesian flow past the wavy bottom [18, 19], as well to wavy tubes [20]. It can work also for the more complete hydrodynamics of Navier-Stokes equations [12, 21]. The applications to the stationary heat conduction [22], and to electrokinetic phenomena in two-dimensional channels [23], are available as well.

In [13] an arbitrary profiles $S^{\pm}(x_1, x_2)$ were explored. It was assumed only that they satisfy some natural conditions, such as

$$|T(x_1, x_2)| \leqslant 1 \quad \text{and} \quad |B(x_1, x_2)| \leqslant 1. \tag{48}$$

The infinite differentiability is assumed for the functions $T(x_1, x_2)$ and $B(x_1, x_2)$. Such assumption was made in order to calculate velocities and permeability, and to solve an emerging cascade of boundary value problems for the Stokes equations in a straight channel [13]. Influence of the curvilinear edges on flow is of significant theoretical interest. It illustrates the mechanism of viscous flow under different geometrical conditions. But the flow through curvilinear channels also finds applications in porous media [11, 24].

To make our paper self-consistent we bring below some general information about the mathematical formulation of the problem and some permeability definitions. Let $\mathbf{u} = \mathbf{u}(x_1, x_2, x_3)$ be the velocity vector, and $p = p(x_1, x_2, x_3)$ the pressure. The flow of a viscous fluid through a channel is considered under condition that the Reynolds number is small and the Stokes flow approximation is valid. The fluid is governed by the Stokes equations

$$\begin{aligned} &\mu \nabla^2 \mathbf{u} = \nabla p, \\ &\nabla \cdot \mathbf{u} = \mathbf{0}, \end{aligned} \tag{49}$$

with the boundary conditions

$$\mathbf{u} = \mathbf{0} \qquad \text{on} \quad S^{\pm}. \tag{50}$$

The solution $\mathbf{u}$ of (49)–(50) is sought within the class of functions periodic with period $2L$ both in variables x_1 and x_2.

Let also u be the x-component of $\mathbf{u}$. Let also an overall external gradient pressure $\overline{\nabla p}$ to be applied along the x_1-direction. It corresponds to a constant jump $2L\overline{\nabla p}$ along the x_1-axis of the periodic cell. Then the permeability of

Preprints (www.preprints.org) | NOT PEER-REVIEWED | Posted: 11 September 2020 doi:10.20944/preprints202009.0141.v2

the channel in the x_1-direction is defined as the result of integration,

$$K_{x_1}(\epsilon) = -\frac{\mu}{\overline{\nabla p}\,|\tau|}\int\limits_{-L}^{L}\int\limits_{-L}^{L} dx_1\,dx_2 \int\limits_{S^-(x_1,x_2)}^{S^+(x_1,x_2)} u(x_1,x_2,x_3)\,dx_3\,. \tag{51}$$

Here $|\tau|$ stands for the volume of the unit cell Q of the channel,

$$|\tau| = \int\limits_{-L}^{L}\int\limits_{-L}^{L} dx_1\,dx_2 \int\limits_{S^-(x_1,x_2)}^{S^+(x_1,x_2)} dx_3\,. \tag{52}$$

The sought $K_{x_1}(\epsilon)$ in (51) is going to be expressed explicitly as a function in ϵ. More precisely, the ratio $K = K(\epsilon)$ of the dimensional permeability for the curvilinear channel and of the Poiseuille flow

$$K(\epsilon) = \frac{K_{x_1}(\epsilon)}{K_{x_1}(0)}, \tag{53}$$

is going to be considered. In the case of $\epsilon = 0$ we return to the familiar Poiseuille flow. For such flow the definition (51) gives the transparent expression for permeability

$$K_{x_1}(0) = \frac{b^2}{3}. \tag{54}$$

I. e., we return to the classical Poiseuille flow in the channel bounded by two parallel planes which arises when a pressure gradient is applied, and the flow profile obeys the parabolic law.

Most important for our methodology, the formula of [13] determines the coefficients of a Taylor expansion for the permeability

$$K(\epsilon) = \sum_{m=0}^{\infty} c_m \epsilon^m.$$

with the normalization (53) used to find K. In practical computations $K(\epsilon)$ is approximated by the truncation, leading to Taylor polynomial of order N

$$K_N(\epsilon) = \sum_{m=0}^{N} c_m \epsilon^m.$$

The domain of application of this formula appears to be restricted. And the corresponding Taylor series are divergent for larger ϵ.

Preprints (www.preprints.org) | NOT PEER-REVIEWED | Posted: 11 September 2020 doi:10.20944/preprints202009.0141.v2

3.1.1 Symmetric sinusoidal two-dimensional channel. Walls can touch

Mityushev, Malevich and Adler in [13], considered the following, bounded two-dimensional channel

$$z = b(1 + \epsilon \cos x) \quad , \quad z = -b(1 + \epsilon \cos x). \tag{55}$$

The expansion for permeability was found up to $O(\epsilon^{32})$, and for $b = 0.5$. This example is popular among the researchers, as is documented in [13]. The following truncated polynomial for the permeability as the function of "waviness" parameter ϵ was presented,

$$\begin{aligned} &K_{30}(\epsilon) = \\ &1 - 3.14963\epsilon^2 + 4.08109\epsilon^4 - 3.48479\epsilon^6 + 2.93797\epsilon^8 - 2.56771\epsilon^{10} + \\ &2.21983\epsilon^{12} - 1.93018\epsilon^{14} + 1.67294\epsilon^{16} - 1.45302\epsilon^{18} + 1.26017\epsilon^{20} - \\ &1.09411\epsilon^{22} + 0.949113\epsilon^{24} - 0.823912\epsilon^{26} + 0.714804\epsilon^{28} - 0.620463\epsilon^{30} \\ &+ O(\epsilon^{32}). \end{aligned} \tag{56}$$

On the other hand, for larger ϵ, a lubrication approximation was discussed in [11]. It is motivated by the solution in the case of two cylinders of different radii that are almost in contact with one another along a line. For equal radii a, the flow rate q per unit length is proportional to the pressure variation Δp

$$q = -\frac{K_l}{\mu}\Delta p, \tag{57}$$

where K_l is given by

$$K_l = \frac{2}{9\pi}\sqrt{\frac{\delta^5}{a}} \tag{58}$$

and δ is the gap between the cylinders. For the channel (55), if ϵ is close to unity, the aperture at $x = -\pi$ is close to zero. Most important, one can apply (58) to the local channel with $\delta = 2b(1-\epsilon)$ and $a = b\epsilon$. As $\epsilon \to \epsilon_c = 1$, simply confronts the following power-law

$$K_l \simeq \frac{8\sqrt{2}\sqrt{b^4}(\epsilon - 1)^{5/2}}{9\pi}. \tag{59}$$

It has the general critical form with the critical index for permeability $\varkappa = 5/2$. The critical amplitude can be extracted as well, so that $A = \frac{8\sqrt{2}b^2}{9\pi}$. In the case under consideration we calculate $A = 0.100035$.

Preprints (www.preprints.org) | NOT PEER-REVIEWED | Posted: 11 September 2020 doi:10.20944/preprints202009.0141.v2

The reasons for failure of lubrication approximation are explained [11, 13] and also in [9]. In a nutshell, the main assumption of the lubrication approximation is that the velocity has a parabolic profile. Even for the plane channels [13], the lubrication approximation gives correct results only for channels in which the mean surface is sufficiently close to a plane and for small value of ϵ.

In what follows we completely avoid the lubrication approximation. The technique of approximants allows to approach the critical region, when the walls nearly touch, only based on the expansion (56). Mind that the problem of interest can be formulated mathematically just as in section 2.

In the concrete case we have the polynomial approximation (56) of the function $K(\epsilon)$. And we intend to to calculate critical index and amplitude(s) of the asymptotically equivalent approximants in the vicinity of the threshold $\epsilon = \epsilon_c = 1$. When such extrapolation problem is solved, one can proceed with an interpolation problem. In the latter case assuming that the critical behavior is known in advance, and derive the compact formula for all ϵ.

Let us calculate the index and amplitude for the critical behavior written in general form

$$K(\epsilon) \simeq A(\epsilon_c - \epsilon)^{\varkappa}, \text{ as } \epsilon \to \epsilon_c - 0 \, . \tag{60}$$

We proceed routinely, in accord with section 2. Let us first apply the transformation,

$$z = \frac{\epsilon}{1-\epsilon} \;\Leftrightarrow\; \epsilon = \frac{z}{z+1},$$

to the series (56). The transformation makes technical application of the different approximants more convenient.

To such transformed series $M_1(z)$ let us apply the $DLog$ transformation and obtain the transformed series $M(z)$. In terms of $M(z)$ one can readily obtain the sequence of Padé approximations $\varkappa_n$ for the critical index $\varkappa$. Namely, we obtain the sequence of values

$$\varkappa_n = -\lim_{z\to\infty}(zPadeApproximant[M[z], n, n+1]). \tag{61}$$

The approximations for the critical index generated by the sequence of Padé approximants, corresponding to their order increasing, converge nicely to the value $5/2$, as shown below,

$$\varkappa_1 = 2.57972, \quad \varkappa_2 = 2.30995, \quad \varkappa_3 = 2.47451, \quad \varkappa_4 = 2.49689,$$

$$\varkappa_5 = 2.4959, \quad \varkappa_6 = 2.49791, \quad \varkappa_7 = 2.49923, \quad \varkappa_8 = 2.50113,$$

Preprints (www.preprints.org) | NOT PEER-REVIEWED | Posted: 11 September 2020 doi:10.20944/preprints202009.0141.v2

$$\varkappa_9 = 2.50028, \varkappa_{10} = 2.49783, \varkappa_{11} = 2.49778, \varkappa_{12} = 2.49829, \varkappa_{13} = 2.49836.$$

If $B_n(z) = PadeApproximant[M[z], n, n+1]$, then one can also find the approximation for permeability

$$K_n^*(\epsilon) = \exp\left(\int_0^{\frac{\epsilon}{\epsilon_c-\epsilon}} B_n(z)\, dz\right), \tag{62}$$

and eventually compute the corresponding amplitude

$$A_n = \lim_{\epsilon\to\epsilon_c} (\epsilon_c - \epsilon)^{-\varkappa_n} K_n^*(\epsilon). \tag{63}$$

There is typical value of amplitude, found e.g., with $A_9 = 3.7758$. It appears to be by order of magnitude larger than the value deduced from the lubrication approximation. Now, let us fix the critical index to the obtained in extrapolation value $5/2$. Now, one can calculate A using the standard Padé technique, finding the value of 3.77188. The latter turns out to be very close to the value just found above from the extrapolation.

The permeability can be expressed rather compactly, in terms of factor approximant, asymptotically equivalent to (56) up to 16th order inclusively,

$$K_{1/2}^*(\epsilon) = \frac{\left(1-\epsilon^2\right)^{2.5}\left(0.239311\epsilon^2+1\right)^{0.591597}}{(1-0.722851\epsilon^2)^{0.00840612}(1-0.260764\epsilon^2)^{0.270545}(0.867799\epsilon^2+1)^{1.00004}}. \tag{64}$$

From (64) we again find the amplitude $A = 3.77177$, and again it turns out to be in line with our estimates.

Still, there are some higher order coefficients, not used in construction of the approximant (64). From the formula (64) one can readily evaluate the higher-order coefficients (56), not employed in the final formula,

$$c_{18} = -1.453, \quad c_{20} = 1.26014, \quad c_{22} = -1.09408, \quad c_{24} = 0.949078,$$
$$c_{26} = -0.823874, \quad c_{28} = 0.714764, \quad c_{30} = -0.620422.$$

Formula (64) appears to be exceptionally successful in reproducing the "unemployed" coefficients in the expansion (56). The maximal error appears in reproducing the $30th$ order, and it equals just 0.0066%.

We illustrate below how lubrication approximation breaks down even in a close vicinity of ϵ_c. In figure 1 formula (64) is compared with both available analytical expression for the asymptotic regimes.

Preprints (www.preprints.org) | NOT PEER-REVIEWED | Posted: 11 September 2020 doi:10.20944/preprints202009.0141.v2

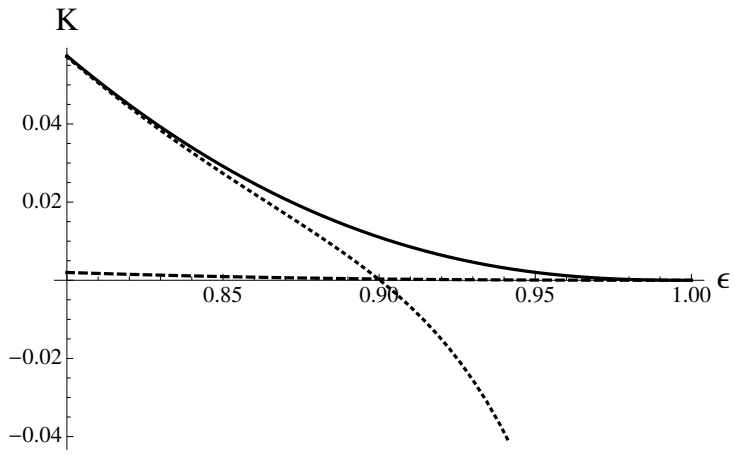

Figure 1: Formula for the factor approximant (64) (solid) is compared with the truncated power series (dotted) and lubrication approximation (dashed)

3.1.2 Symmetric sinusoidal two-dimensional channel. Example 2

Let us again consider the channel bounded by the surfaces (55), but with different parameter, $b = 0.25$. The truncated polynomial $K(\epsilon)$ was obtained in [13] as well,

$$\begin{aligned} &K(\epsilon) = \\ &1 - 3.03748\epsilon^2 + 3.54570\epsilon^4 - 2.33505\epsilon^6 + 1.35447\epsilon^8 - 0.83303\epsilon^{10} \\ &+0.49762\epsilon^{12} - 0.30350\epsilon^{14} + 0.18185\epsilon^{16} - 0.11083\epsilon^{18} + 0.06636\epsilon^{20} \\ &-0.04051\epsilon^{22} + 0.02419\epsilon^{26}0.00880\epsilon^{28} - 0.00544\epsilon^{30} + \\ &O(\epsilon^{32}). \end{aligned} \tag{65}$$

Again, just like in previous example, there is an excellent convergence within the approximations for the critical index. They were generated by the sequence of Padé approximants using formula (61),

$$\varkappa_1 = 2.64456, \quad \varkappa_2 = 2.41346, \quad \varkappa_3 = 2.49488, \quad \varkappa_4 = 2.49992,$$

$$\varkappa_5 = 2.49991, \quad \varkappa_6 = 2.50026, \quad \varkappa_7 = 2.50068, \quad \varkappa_8 = 2.50087,$$

$$\varkappa_9 = 2.50086, \quad \varkappa_{10} = 2.50063, \quad \varkappa_{11} = 2.50063, \quad \varkappa_{12} = 2.50086,$$

$$\varkappa_{13} = 2.50087, \quad \varkappa_{14} = 2.50068, \quad \varkappa_{15} = 2.50026.$$

Preprints (www.preprints.org) | NOT PEER-REVIEWED | Posted: 11 September 2020 doi:10.20944/preprints202009.0141.v2

Evidently this sequence leads to the same value for the index, $\varkappa = 5/2$. The value of amplitude is estimated as well, as $A_{15} = 3.77362$. Both amplitude and index appear to be independent on b, suggesting an universal regime in the vicinity of ϵ_c.

Interpolating with the known critical index, one can calculate the amplitude A, using standard Padé technique, finding again the very close value of $A \approx 3.77316$. As above, the permeability can be expressed compactly as factor approximant,

$$K^*_{1/4} = \frac{(1-\epsilon^2)^{2.5}}{(1-0.0437141\epsilon^2)^{1.37166}\,(0.606745\epsilon^2+1)^{0.984665}}. \qquad (66)$$

The amplitude can be calculated as $A = 3.77062$. And once again, it appears to be by orders of magnitude larger than the value 0.02501, estimated from the lubrication theory. From the crossover formula (66) one can readily obtain the higher-order coefficients (65), not employed in the derivation. Formula (64) appears to be accurate enough in reproducing the coefficients in the expansion (56), not employed in its construction. The maximal error is in reproducing c_{30}, and it is equal to 2.147%.

In figure 2, the formula (66) is compared with analytical expressions available in both asymptotic regimes. The amplitude and overall behavior of permeability in the vicinity of ϵ_c, practically does not depend on the parameter b. One can think that some universal (not dependent on b) mechanism is at work here. The chief suspect to be approached is celebrated similarity-solutions with complex exponent, known as viscous Moffat eddies [26]. Obviously they are not covered by the lubrication theory [25]. Eddies manifest themselves as reversed-flow regions near the walls. Onset of eddies is expected in the vicinity of ϵ_e, corresponding to zero of the polynomial approximations (64), (66). The onset of eddies would lead to a total disappearance of permeability. We believe it to be an artifact, being corrected by a detailed consideration of the region $\epsilon \sim 1$ with a power-law ansatz. As the value of b decreases, the value of ϵ_e moves closer to ϵ_c.

3.1.3 Parallel sinusoidal two-dimensional channel. Walls not touching

Let us proceed with the case principally different from the two cases just studied. Consider the channel bounded by the surfaces

$$z = b(1+\epsilon\cos x)\,, \quad z = -b(1-\epsilon\cos x)\,, \qquad (67)$$

Preprints (www.preprints.org) | NOT PEER-REVIEWED | Posted: 11 September 2020 doi:10.20944/preprints202009.0141.v2

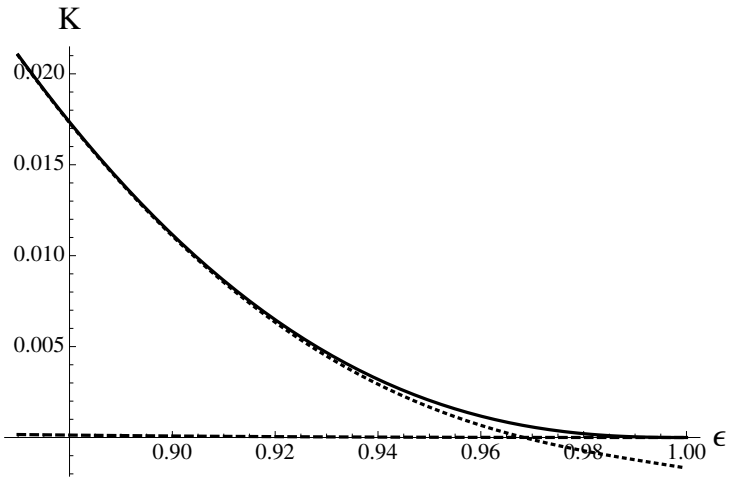

Figure 2: Formula (66) (solid) is compared with the truncated polynomial (dotted) and lubrication formula (dashed)

with $b = 0.5$ [13]. There is no possibility of the walls touching and permeability remains finite but expected to decay as a power-law as ϵ becomes large. Instead of a critical transition from permeable to non-permeable phase, we have a non-critical transition, or crossover as defined in [27]. The crossover is from high-to low permeability, and unravels with increasing parameter ϵ. The crossover can be still characterized by the power-law, as one can study corresponding critical index at large ϵ. Eddies are not expected in such channel even for very large ϵ [13]. But for large b eddies are not excluded [13]

The truncated series for permeability is calculated up to $O(\epsilon^{32})$,

$$
\begin{aligned}
&K_{30}(\epsilon) = \\
&1 - 2.53686\times10^{-1}\epsilon^2 + 4.28907\times10^{-2}\epsilon^4 - 5.46188\times10^{-3}\epsilon^6 \\
&+4.54695\times10^{-4}\epsilon^8 + 9.0656\times10^{-6}\epsilon^{10} - 1.41572\times10^{-5}\epsilon^{12} + 3.76584\times10^{-6}\epsilon^{14} \\
&-6.72021\times10^{-7}\epsilon^{16} + 7.58331\times10^{-8}\epsilon^{18} + 2.34495\times10^{-9}\epsilon^{20} - 4.59993\times10^{-9}\epsilon^{22} \\
&+1.88446\times10^{-9}\epsilon^{24} - 8.6005\times10^{-11}\epsilon^{26} + 3.34156\times10^{-9}\epsilon^{28} + 1.63748\times10^{-9}\epsilon^{30}.
\end{aligned}
\tag{68}
$$

In this case it is well understood, that the velocity is analytic in ϵ in the disk $|\epsilon| < \epsilon_0$. Therefore, one can deduce that (68) is valid for $\epsilon < \epsilon_0$, where ϵ_0 is of order $\frac{1}{b\chi}$, with χ being the maximal wave number of $T(x_1, x_2)$ and $B(x_1, x_2)$.

Still, in order to extend $K(\epsilon)$ for $\epsilon \geqslant \epsilon_0$, one can apply Padé approximation to the polynomial (68), which agrees with it up to $O(\epsilon^{32})$. The Padé

Preprints (www.preprints.org) | NOT PEER-REVIEWED | Posted: 11 September 2020 doi:10.20944/preprints202009.0141.v2

approximant of the order $(10, 20)$ was first developed in [13],

$$K_{10,20}(\epsilon) = \frac{P_{10}(\epsilon)}{Q_{20}(\epsilon)}, \tag{69}$$

where

$$\begin{aligned} &P_{10}(\epsilon) = 1 - 3.14215\epsilon^2 + 6.59346\epsilon^4 + 34.7591\epsilon^6 + 13.3065\epsilon^8 + 1.53446\epsilon^{10}, \\ &Q_{20}(\epsilon) = 1 - 2.88846\epsilon^2 + 5.81781\epsilon^4 + 36.3643\epsilon^6 + 22.2659\epsilon^8 + 5.65641\epsilon^{10} \\ &+0.675967\epsilon^{12} + 0.033858\epsilon^{14} + 0.000131\epsilon^{16} - 0.000010\epsilon^{18} + 0.000001\epsilon^{20}. \end{aligned} \tag{70}$$

This approximant finds that $K_{10,20}(\epsilon) \sim \epsilon^{-10}$, as $\epsilon \to \infty$.

In such spirit, one can think that the permeability decays as $K(\epsilon) \sim \epsilon^{\nu}$, as $\epsilon \to \infty$, The index ν can be obtained as the limit

$$\nu = \lim_{\epsilon \to \infty} \epsilon \, \frac{d}{d\epsilon} \, \log K(\epsilon) \, . \tag{71}$$

as explained in the section 2.

Assuming that the small-variable expansion for the function is given by the truncated sum $K_{tr}(\epsilon)$, as in (68), we have the corresponding small-variable expression $N(\epsilon)$ for the effective critical exponent which equals $\epsilon \, \frac{d}{d\epsilon} \, \log K_{tr}(\epsilon)$. By applying to the obtained series $N(\epsilon)$ the method of Padé approximants, as has been discussed above, the sought approximate expression for the critical exponent is obtained,

$$\nu_k = \lim_{\epsilon \to \infty} \epsilon P_{k,k+1}(\epsilon) \, , \tag{72}$$

dependent on the approximation order k. Application of the method to the truncated series (68), is straightforward and suggests strongly the value of $\nu = -4$, as can be seen from Figure 3. The amplitude B, corresponding to $k = 14$, is equal to 44.5872. Assume now that $\nu = -4$, and construct the sequence of Padé approximants $P_{n,n+4}$, which lead to such index by design. There is a convergence in the approximation sequence for the amplitude B. One can safely assume that it converges to the value of 43.2. The sequence is shown in Fig. 4.

based on the behavior of the amplitude, for the permeability we suggest the Padé approximant of the order $(12, 16)$,

$$K_{12,16}(\epsilon) = \frac{P_{12}(\epsilon)}{Q_{16}(\epsilon)}, \tag{73}$$

Preprints (www.preprints.org) | NOT PEER-REVIEWED | Posted: 11 September 2020 doi:10.20944/preprints202009.0141.v2

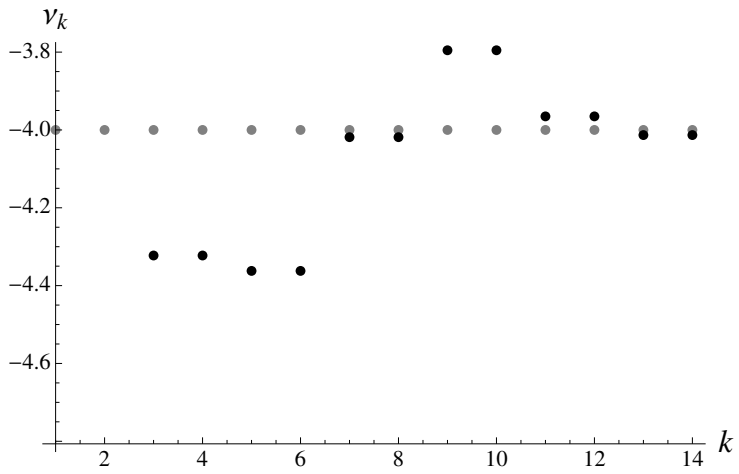

Figure 3: The index ν at infinity, is shown dependent on approximation number k. The values found by computing (72), are shown with black circles. They are compared with the most plausible value of -4 (shown with gray circles).

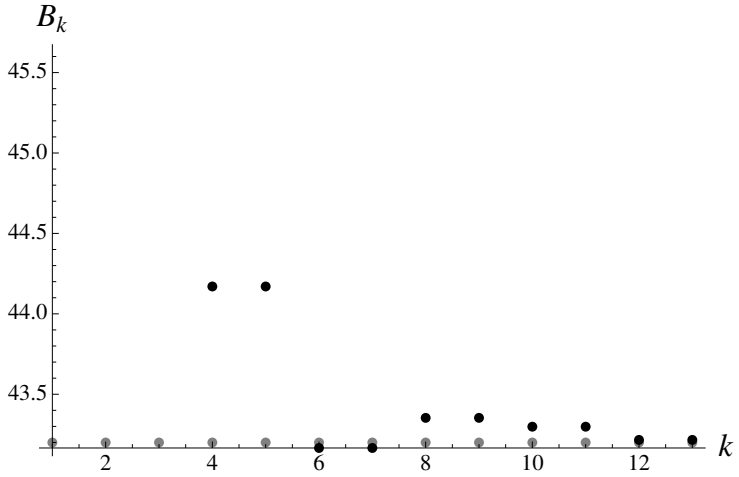

Figure 4: The amplitude B dependence on approximation number k is shown with black circles. One can see the convergence to the value of 43.2, shown with squares.

Preprints (www.preprints.org) | NOT PEER-REVIEWED | Posted: 11 September 2020 doi:10.20944/preprints202009.0141.v2

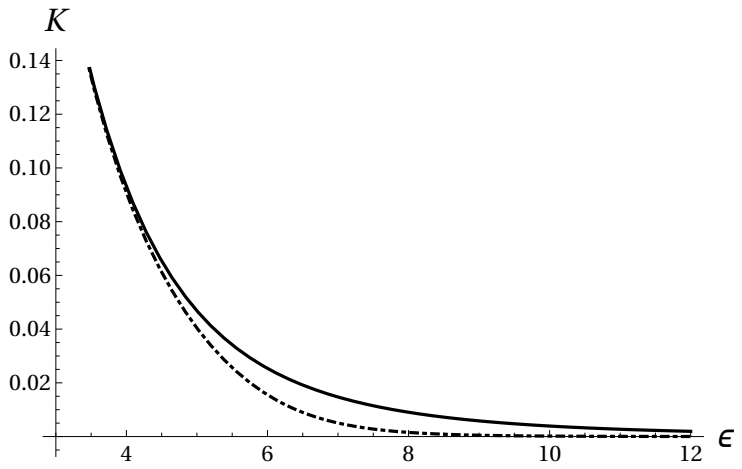

Figure 5: The two different Padé approximants for permeability, $K_{10,20}$ (dot-dashed) and $K_{12,16}$ (solid) are compared.

where

$$\begin{array}{l} P_{12}(\epsilon) = 1 - 5.86404\epsilon^2 - 3.84897\epsilon^4 + 1.12295\epsilon^6 + 0.867771\epsilon^8 + \\ 0.151922\epsilon^{10} + 0.00735283\epsilon^{12}, \\ Q_{16}(\epsilon) = 1 - 5.61035\epsilon^2 - 5.31512\epsilon^4 + 0.0206681\epsilon^6 + 1.06989\epsilon^8 + \\ +0.395962\epsilon^{10} + 0.0645092\epsilon^{12} + 0.0051812\epsilon^{14} + 0.000170141\epsilon^{16}. \end{array} \tag{74}$$

The two Padé approximants are presented, and the effect of arising from the different estimates for the index, could be seen in Fig.5. The permeability can be interpolated also by means of the factor approximant of low order, which "consumes" asymptotic terms only up to the $14th$ order,

$$\begin{array}{l} \mathcal{F}^*_{14}(\epsilon) = \\ (1 + (0.0925028 - 0.0501527i)\epsilon^2)^{-0.957209-0.738327i} \times \\ (1 + (0.0925028 + 0.0501527i)\epsilon^2)^{-0.957209+0.738327i} \times \\ (1 + (0.218267 - 0.101021i)\epsilon^2)^{-0.042791+0.0798889i} \times \\ (1 + (0.218267 + 0.101021i)\epsilon^2)^{-0.042791-0.0798889i}. \end{array} \tag{75}$$

It appears to be very close to $K_{12,16}$, giving a testimony on the high-quality of the original series. The factor approximant (75) may be considered as "smart". It means that it can predict three more coefficients, a_{16}, a_{18}, a_{20}, with average accuracy better than 1%. From (75) one can evaluate the

Preprints (www.preprints.org) | NOT PEER-REVIEWED | Posted: 11 September 2020 doi:10.20944/preprints202009.0141.v2

amplitude $B = 43.3$. The value appears to be in agreement with other estimates found above. Mind that the condition $\nu = -4$ was imposed in the course if derivation of the factor approximant (75). Alternatively, one van try to evaluate the index with factor approximant. To this end one can input one more term from the expansion. After some calculations one finds the index with rather good estimated index, $\nu \approx -4.02$.

3.2 Symmetric sinusoidal three-dimensional channel. Estimates for the two-fluid model

Following [13] let us consider the three-dimensional channel restricted by the surfaces

$$z = \pm b\Big(1 + \frac{1}{2}\epsilon\big(\cos(x+y) + \cos(x-y)\big)\Big), \tag{76}$$

with $b = 0.3$. The permeability is calculated up to $O(\epsilon^{14})$

$$\begin{aligned} K_{14}(\epsilon) = 1 - 0.465674\epsilon^2 + 0.329218\epsilon^4 - 0.261666\epsilon^6 - 0.004467\epsilon^8 - \\ 0.0386987\epsilon^{10} - 0.0177808\epsilon^{12} - 0.0239319\epsilon^{14}. \end{aligned} \tag{77}$$

The case appears to be different from all two-dimensional examples studied above in great detail. For $\epsilon = \epsilon_c = 1$, the surfaces (76) start touching but the permeability remains finite at ϵ_c. The truncated series for permeability (77) is obtained with numerical precision of 10^{-3} for values of ϵ up to 0.61. The permeability at ϵ_c is remains quite significant, $K_{14}(\epsilon_c) = 0.517$, as is simply estimated from the series (77).

One can simply apply the diagonal Padé approximants to the polynomial (77). The Padeé approximants bring the following close results

$$P_{6,6}(\epsilon_c) = 0.51277,\ P_{8,8}(\epsilon_c) = 0.490636.$$

The higher order Padé approximants are readily obtained as well,

$$\begin{aligned} P_{6,6}(\epsilon) &= \tfrac{-0.272534\epsilon^6+0.22825\epsilon^4-0.657553\epsilon^2+1}{-0.0363255\epsilon^6-0.190321\epsilon^4-0.191879\epsilon^2+1}; \\ P_{8,8}(\epsilon) &= \tfrac{-0.266547\epsilon^8-0.131478\epsilon^6-0.363105\epsilon^4+0.256413\epsilon^2+1}{-0.0832011\epsilon^8-0.273346\epsilon^6-0.356065\epsilon^4+0.722087\epsilon^2+1}. \end{aligned} \tag{78}$$

One can deduce a reasonable bounds for the solution, such as the upper and lower Padé bounds for $P_{6,6}(\epsilon)$ [1]. They are are given by the non-diagonal Padé approximants [1],

$$\begin{aligned} P_{6,4}(\epsilon) &= \tfrac{-0.25985\epsilon^6+0.27733\epsilon^4-0.664548\epsilon^2+1}{-0.144498\epsilon^4-0.198874\epsilon^2+1}; \\ P_{6,8}(\epsilon) &= \tfrac{-0.354713\epsilon^6+0.280003\epsilon^4-0.721617\epsilon^2+1}{-0.0476736\epsilon^8-0.0872062\epsilon^6-0.168401\epsilon^4-0.255943\epsilon^2+1}. \end{aligned} \tag{79}$$

Preprints (www.preprints.org) | NOT PEER-REVIEWED | Posted: 11 September 2020 doi:10.20944/preprints202009.0141.v2

With such guidance we can construct and evaluate the two factor approximants. The first one, $\mathcal{F}^*_{12}(\epsilon)$, is completely standard, while the second, $\mathcal{F}^*_{12,s}(\epsilon)$, is "shifted". The shift also can calculated and employed to estimate the sought value,

$$\begin{array}{l} \mathcal{F}^*_{12}(\epsilon) = (1 - 0.867964\epsilon^2)^{0.474676} \times \\ (1 + (0.0821614 + 0.533783i)\epsilon^2)^{1.35488+0.258822i} \times \\ (1 + (0.0821614 - 0.533783i)\epsilon^2)^{1.35488-0.258822i}; \\ \\ \mathcal{F}^*_{12,s}(\epsilon) = 0.481814 + 0.518186\,(1 - \epsilon^2)^{0.766642} \times \\ (1 - (0.074165 + 0.649541i)\epsilon^2)^{1.46148+0.0652476i} \times \\ (1 - (0.074165 - 0.649541i)\epsilon^2)^{1.46148-0.0652476i}. \end{array} \tag{80}$$

As usual we are looking for the permeability at $\epsilon = 1$. Thus, we have three estimates,

$$P_{6,6}(1) = 0.51277, \quad F^*_{12}(1) = 0.50195, \quad F^*_{12,s}(1) = 0.481814,$$

all satisfying the given bounds. Their average K_{av} is equal to 0.498845, and corresponding margin of error can be estimated through the variance, which equals 0.0128272. Different formulas for the permeability together with bounds, are compared in in Fig.6.

Close to ϵ_c we evaluate that

$$P_{6,6}(\epsilon) \simeq 0.51277 + 2.30175(1 - \epsilon),$$

and the correction to constant is linear. As well, one can calculate from the shifted factor approximant, that

$$\mathcal{F}^*_{12,s}(\epsilon) \simeq 0.481814 + 1.36825(1 - \epsilon)^{0.766642}.$$

Possibly, we have here an indication of a non-trivial subcritical index with the value of 0.767.

To elaborate further, we would like to study in more detail the behavior of permeability in the vicinity of ϵ_c. Assuming also some deviations from linearity, motivated by the shifted factor approximant.

We can start with general initial approximation for the permeability, which holds in the vicinity of $\epsilon_c = 1$,

$$K_0(\epsilon) \simeq A_0 + A_1(\epsilon_c^2 - \epsilon^2)^{\lambda_0}, \tag{81}$$

Preprints (www.preprints.org) | NOT PEER-REVIEWED | Posted: 11 September 2020 doi:10.20944/preprints202009.0141.v2

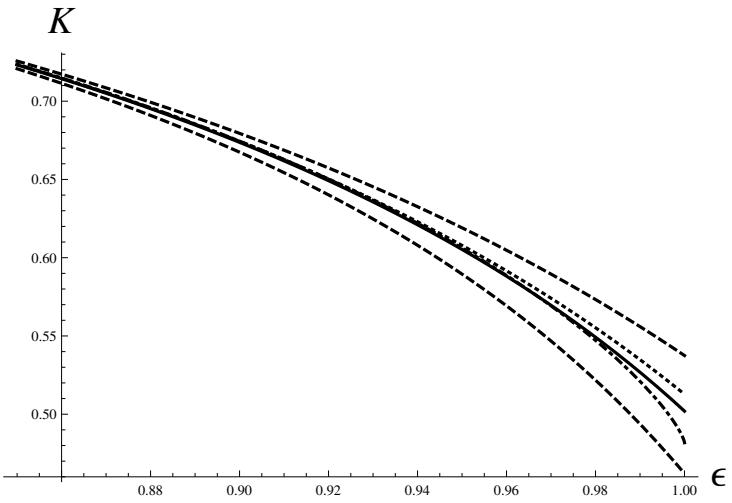

Figure 6: Bounds (79) for the permeability are shown with dashed lines. Comparison of the formulas in the vicinity of ϵ_c: Padé approximant $P_{6,6}$ is shown with with dotted line, factor approximant $\mathcal{F}^*_{12}$ from (80) is shown with solid line, and shifted factor approximant $\mathcal{F}^*_{12,s}$ from (80) is shown with dot-dashed line.

Preprints (www.preprints.org) | NOT PEER-REVIEWED | Posted: 11 September 2020 doi:10.20944/preprints202009.0141.v2

To simplify the procedure of finding the unknowns, let us set from the start $A_0 = K_{av}$. Now, to obtain the remaining unknowns, we can try to satisfy the expansion (77) in the second order. Then, it appear that $A_1 = 0.501155$, $\lambda_0 = 0.929201$. The expression (81) can be understood as a two-fluid model, reflecting on the fact that there are two components in the flow. One which is getting blocked by the obstacles to flow, and another, which can not be blocked.

One ought to appreciate that (81) with its parameters is only a crude approximation. In what follows let us attempt to correct the formula $K_0(\epsilon)$, even further. To this end let us assume in place of λ_0, even some more general functional dependence $\Lambda^*(\epsilon)$. As $\epsilon \to \epsilon_c$, $\Lambda^*(\epsilon) \to \lambda_c$, the sought corrected value. The function $\Lambda^*(\epsilon)$ will be designed in such a way, that it smoothly interpolates between the initial value λ_0 valid at small ϵ, and the sought value λ_c valid as $\epsilon \to \epsilon_c$. The permeability $K^*(\epsilon)$ is getting "dressed" in such way. it is is now given as follows:

$$K^*(\epsilon) = A_0 + A_1(\epsilon_c^2 - \epsilon^2)^{\Lambda^*(\epsilon)}. \tag{82}$$

It should become valid for all ϵ. From (82) one can express $\Lambda^*(\epsilon)$ formally, bearing in mind that we do not have the expression for $K^*(\epsilon)$. All we can do is to use its asymptotic form (77), then express $\Lambda^*(\epsilon)$ as a truncated series for small ϵ. And then we can apply to such obtained series some resummation procedure (e.g. Padé technique). Such resummation is expected to extend the series to the whole region of ϵ. Finally, we are in a position to calculate the limit of the approximants as $\epsilon \to \epsilon_c$, and find the corrected value as $\lambda_c = \Lambda^*(\epsilon_c)$.

Let $p(\epsilon) = K_{14}(\epsilon)$ stand for an asymptotic form of $K^*(\epsilon)$ for small ϵ. Corresponding asymptotic expression for Λ^*, just called $\Lambda(\epsilon)$, can be made explicit from the following relation,

$$\Lambda(\epsilon) \simeq -\frac{\log\left(\frac{(A_0 - p(\epsilon))}{A_1}\right)}{\log(\epsilon_c^2 - \epsilon^2)}. \tag{83}$$

$\Lambda(\epsilon)$ can be explicitly presented as expansion in powers of ϵ around the value of λ_0,

$$\Lambda(\epsilon) = \lambda_0 + \Lambda_1(\epsilon). \tag{84}$$

And only now one can construct a sequence of diagonal Padé approximants

$$\Lambda_n(\epsilon) = \lambda_0 + PadeApproximant[\Lambda_1[\epsilon], n, n]), \tag{85}$$

Preprints (www.preprints.org) | NOT PEER-REVIEWED | Posted: 11 September 2020 doi:10.20944/preprints202009.0141.v2

and find the sought limit $\Lambda^*(\epsilon)$. Finally, we estimate the critical index $\lambda_c = \Lambda^*(\epsilon_c)$ and also find the complete formula for permeability, returning to the expression (82).

There is a good convergence within the approximations for the λ_c generated by the sequence of Padé approximants,

$$\lambda_{c,1} = 0.929201, \quad \lambda_{c,2} = 0.402904, \quad \lambda_{c,4} = 0.631631,$$

$$\lambda_{c,6} = 0.630229, \quad \lambda_{c,8} = 0.702766, \quad \lambda_{c,10} = 0.698385 \quad \lambda_{c,12} = 0.702563.$$

Remarkably, in the highest orders (up to 18-th) the value of index remains practically the same. The final estimate for λ_c can be conjectured to be rational $\frac{2}{3}$.

The function $\Lambda^*(\epsilon)$ is needed to reconstruct the permeability. It can be straightforwardly expressed as the Padé approximant. The approximant corresponding to $\lambda_{c,6}$ has the following form,

$$K_6^*(\epsilon) = 0.498845 + 0.501155\left(1-\epsilon^2\right)^{\frac{-4.15886\epsilon^6+6.957\epsilon^4-7.18244\epsilon^2+0.929201}{-1.56421\epsilon^6+2.06925\epsilon^4-6.98732\epsilon^2+1}}. \quad (86)$$

Formula (86), as well as the higher-order approximant (87), corresponding to $\lambda_{c,8}$,

$$K_8^*(\epsilon) = 0.498845 + 0.501155\left(1-\epsilon^2\right)^{\frac{0.134578\epsilon^8-0.22113\epsilon^6+0.650924\epsilon^4-0.904689\epsilon^2+0.929201}{-0.0295078\epsilon^8-0.199491\epsilon^6+0.298201\epsilon^4-0.23125\epsilon^2+1}}, \quad (87)$$

are confidently located within the Padé-bounds (79). Formulas for the permeability including the subcritical regime, are shown together with bounds in Fig.7. We summarize, that in the case of channel with wavy walls, the lubrication approximation works poorly. The exceptions can be found when the surfaces are sufficiently close to a plane and for small value of ϵ. Different approximation technique, not involving lubrication approximation in any sense, is suggested. Closed-form expressions for arbitrary ϵ are derived for the situations, when walls can or cannot touch. In the former case the critical exponents and amplitudes are calculated without involving the lubrication approximation. In the latter case we anticipate and describe the crossover form the high-permeable to low-permeable state of the channel. it is characterized with the power low. The corresponding critical exponent ν for large ϵ, is found by various techniques. Tiny viscous eddies dominate in this case. Their onset over the whole length of the channel explains the quantitative breakdown of the lubrication approximation for the macroscopic

Preprints (www.preprints.org) | NOT PEER-REVIEWED | Posted: 11 September 2020 doi:10.20944/preprints202009.0141.v2

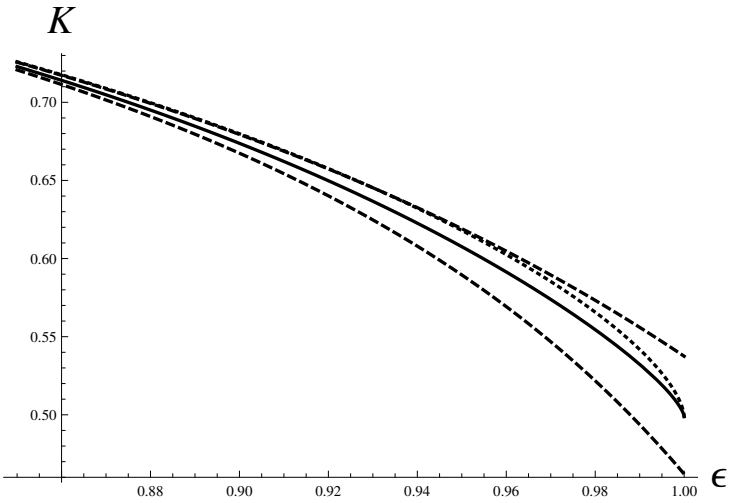

Figure 7: Bounds (79) for the permeability are shown with dashed lines. Comparison of the formulas in the vicinity of ϵ_c: $K_6^*(\epsilon)$ is shown with dotted line, $K_8^*(\epsilon)$ is shown with solid line.

permeability (59). For the important case of a symmetric sinusoidal three-dimensional channel we discuss possibility of a nontrivial sub-critical index. Plausible estimates of its value as found, by developing special technique for such situation.

4 Relaxation phenomena in time series

For the phenomenon to occur, the basic underlying symmetry must be broken. While studying the phenomenon it is important to distinguish between an explicit symmetry breaking when governing equations are not invariant under the desired symmetry and spontaneous symmetry breaking, without presence of any asymmetric cause [29]. When successful, the approach based on broken global symmetries leads to understanding of the key phenomena of magnetism, superconductivity and superfluidity. On the other hand, when some global inherent symmetry can be recognized in physical quantities, we arrive to gloriously successful theory of critical phenomena and vital extensions of perturbation results in quantum field theories, jointly called renormalization group (RG). In a nutshell, we suggest below how to apply

Preprints (www.preprints.org) | NOT PEER-REVIEWED | Posted: 11 September 2020 doi:10.20944/preprints202009.0141.v2

symmetry considerations to the crashes which occur in time series, with most notable example given by stock market crashes.

Assume that numerical data on the time series variable (e.g., price) s is given for some time t segment. Typically, one considers $N+1$ values $s(t_0), s(t_1) \ldots, s(t_N)$, for $N+1$ given at equidistant successive moments in time $t = t_j$, with $j = 0, 1, 2 \ldots, N$ [35].

In time series, one is interested in the extrapolated to future value of s. In financial mathematics, one is particularly interested in the predicted value of log return [35, 38],

$$R(t_N + \delta t) = \ln\left(\frac{s(t_N + \delta t)}{s(t_N)}\right). \tag{88}$$

One can see from the definition that we are really interested in the quantity $\mathbf{S} = \ln(s)$, to be called return. Let us place origin at the very beginning of the time interval, setting also $t_0 = 0$. Naturally, one is interested in the value of $\mathbf{S}(t_N + \delta t)$, allowing to find $R(t_N + \delta t)$ at a later time. Since the approach developed in [35, 28], is invariant with regard to the time unit choice, we consider temporal points of the data set as integer, while consider the actual time variable as continuous.

Modern physics when applied to financial theory is concerned with ergodicity violations [30, 31, 32, 33]. Ergodicity violations may be understood as a manifestation of a non-stationarity, or violation of time-invariance of random process. Metastable phases in condensed matter also defy ergodicity over long observation timescales. In special quantum systems of ultracold atoms spontaneous breaking of time-translation symmetry causes the formation of temporal crystalline structures [34]. Concept of a spontaneously broken time-translation invariance can be useful for time series in application to market dynamics as first suggested in [35]. According to [35], window of forecasting of time series describing market evolution emerges due to a spontaneous breaking/restoration of the continuous time-translation invariance, dictated by relative probabilities of the evolution patterns [36]. In turn, the probabilities are derived from the stability considerations.

Notion of probability introduced in [36] is not based on the same conventional statistical ensemble probability for a collection of people, but is closer to the time probability, concerned with a single person living through time, see Gell-Mann, Peters [32], Taleb [33]. Probabilistic trading patterns correspond to local breakdown of time-translation invariance. Their evolution leads to the time-translation symmetry complete (or partial) restoration. We

Preprints (www.preprints.org) | NOT PEER-REVIEWED | Posted: 11 September 2020 doi:10.20944/preprints202009.0141.v2

need to estimate typical time, amplitude and direction for such restorative process. Thus we are not confined to a binary outcome as in [35], but attempt to estimate also the magnitude of the event.

A catastrophic downward acceleration regime in the time series is known as crash [39]. Time series representing market price dynamics in the vicinity of crisis (crash, melt-up), could be treated as a self-similar evolution, because of prevalence of the collective coherent behavior of many trading, interacting agents [36, 40], including humans and machine algorithms. The dominant collective slow mode corresponding to such behavior, develops according to some law, formalized as a time-invariant, self-similar evolution. Away from crisis there is a superposition of collective coherent mode (generalized trend) and of a stochastic incoherent behavior of the agents [36, 38]. We do not attempt here to write down a generic evolution equation of behind the time series pertaining to market dynamics. Instead. we consider, locally in time, some trial functions-approximants, in the form inspired by the solutions to some well-known evolution equations. The approximants are designed to respect or violate the self-similarity. Our goal here is not of forecasting/timing the crash, but studying the crash as particular phenomenon created by spontaneous, time-translation symmetry breaking/restoration.

Since the market dynamics is believed to be formed by a crowd (herd) behavior of many interacting agents, there are ongoing attempts to create empirical, binary-type prediction markets functioning on such principle, or mini Wall Streets [37]. Prediction markets often work pretty well, however there are many cases when they give wrong prediction or make any prediction at all. Such special set-ups are already very useful in reaching understanding that market crowds are correct only if they express a sufficient diversity of opinion. Otherwise, market crowd can have a collective breakdowns, i.e., is fallible as expected by Soros [39].

4.0.1 Self-similarity and time translation invariance

According to Isaac Newton and Murray Gell-Mann, the laws of nature are somehow self-similar. The laws of Newtonian mechanics are invariant with respect to Galilean group, expressing Galileo's principle of relativity [42],. The group includes time-translation invariance. Or else, the laws of classical mechanics are self-similar. What should be the underlying symmetry for price dynamics? In normal times the average price trajectory is exponential, because of the compounding interests, and we enjoy an almost constant

Preprints (www.preprints.org) | NOT PEER-REVIEWED | Posted: 11 September 2020 doi:10.20944/preprints202009.0141.v2

return (or price growth rate) [43].

Indeed, let s_{t_0} be an underlying security (index) price at $t = t_0$. Let F_t^P be the fair value of the future requiring a risk associated expected return β [33]. Then (see, e.g.,[33]), expected forward price $F_t^P = s_{t_0} \exp(\beta(t - t_0)$. For example, a share of a stock would be correctly priced with the expected return calculated as the return of a risk-free money market fund minus the payout of the asset, being a continuous dividend for a stock [33]. Thus, rather simple and natural exponential estimates are constantly made for the stocks and alike. The formula forward price is self-similar, or time-translation invariant, as explained below.

However, as noted in [39, 43], prices often significantly deviate from such simple description. Bubbles can be formed, as well as other presumed patterns of technical analysis. Asset prices strongly deviate from the fundamental value over significant intervals of time. The fundamental value is not truly observable, making definition of such intervals somewhat elusive. There are very real mechanisms in work, acting to increase and even accelerate the deviation from fundamental value. The causes of deviation could be "option hedging, portfolio insurance strategies, leveraging and margin requirements, imitation and herding behavior ", as is the authoritative opinion expressed in [39, 43].

Recall also that meaningful technical analysis starts from from recasting the time series data using some polynomial representation to serve as the expansion [35]. The regression is constructed in standard fashion by minimizing mean-square deviation, with the effective result that the high-frequency component of the price is getting average out. Then one can consider self-similarity in averages [40]. Indeed, the standard polynomial regressions are invariant under time-translation, retaining their form after arbitrary selection of origin of time with simple redefinition of all parameters. We put forward the idea that it is onset of broken time-translation invariance that signifies birth of a bubble, or of some other temporal pattern preceding crash. End of pattern corresponds to the restoration of time-translation invariance, partially or fully. Our task is to express this idea in quantitative terms by making explicit transformation from the regression-based technical analysis to the valuation formula in the exponential form, bearing in mind taking into account strong deviations from the standard valuation formulae.

Assume that a time series dynamics is predominantly governed by its own internal laws. This is the same as to write down a self-similar evolution for

Preprints (www.preprints.org) | NOT PEER-REVIEWED | Posted: 11 September 2020 doi:10.20944/preprints202009.0141.v2

the marker price s [44], meaning that for arbitrary shift τ one can see that

$$s(t+\tau, a) = s(t, s(\tau, a)), \tag{89}$$

with the initial condition $s(0, a) = a$ [45, 46]. The value of the self-similar function s in the moment $t + \tau$ with given initial condition, is the same as in the moment t, with the initial condition shifted to the value of s in the moment τ.

When t stands for true time, the property of self-similarity means the time-translation invariance. Formally understood equation (89) gives a background for the field-theoretical renormalization group, with addition of some perturbation expansion for the sought quantity, which should be resummed in accordance with self-similarity expressed in the form of ODE [45, 46, 47]. The time-translation invariance expressed by (89), means that the law for price evolution exists and remains unchanged with time, with proper transformation of the initial conditions [42]. The role of expansion when price dynamics is concerned, is accomplished by meaningful technical analysis, by recasting data in the form of some polynomial representation [35].

Consider first the simplest case of technical analysis. The linear function can be formally considered as the function of time and initial condition a, namely $s_1(t, a) = a + bt$, and $s_1(0, a) = a$. The linear function (regression) is self-similar, or time-translation invariant, as can be checked directly, by substitution to (89).

Through some standard procedure let us obtain the linear regression on the data around the origin $t_0 = 0$, so that

$$s_{0,1}(t) = a_1 + b_1 t.$$

Note that the position of origin is arbitrary, and it can be mode to arbitrary position given by real number r, so that

$$s_{r,1}(t) = A_1(r) + B_1(r)(t - r),$$

with new and different coefficients. It turns out that the coefficients are related as follows

$$A_1(r) = a_1 + b_1 r, \;\; B_1(r) = b_1,$$

so that

$$s_{r,1}(t) \equiv s_{0,1}(t).$$

Preprints (www.preprints.org) | NOT PEER-REVIEWED | Posted: 11 September 2020 doi:10.20944/preprints202009.0141.v2

By shifting origin we created an r-dependent form of the linear regression $s_{r,1}$, which can be used constructively. Thus instead of a single regression we have its r-replicas, equivalent to the original form of regression, and all replicas respect time-translation symmetry. In such sense one can speak about replica symmetry. Of course, we would like to avoid such redundancy in data parametrization.

The position of origin in time can be explicitly introduced into the regression formula and included into the coefficients, but actual results of calculations with any arbitrary chosen origin will remain the same. Such property can be expressed as some symmetry. However, intuitively, one would expect that the result of extrapolation with chosen predictors should be dependent on the point of origin r. Indeed, various patterns such as "heads and shoulders", "cup-with-handle"," hockey stick", etc., considered by technical analysts do depend on where the point of origin is placed. In physics, the point of origin (Big Bang) plays a fundamental role. We should find the way to break the replica symmetry.

As discussed above it is exponential shapes that are natural in pricing. Exponential function

$$E(t,a) = a\exp(\beta t),$$

with initial condition a and arbitrary β, satisfy functional self-similarity as well. It can be replicated as

$$\begin{aligned} E_r(t) &= \alpha(r)\exp(\beta(t-r)),\\ \alpha(r) &= a\exp(\beta r). \end{aligned} \tag{90}$$

Having β dependent on r is going to *violate* the time-translation and replica symmetry. Instead of a global time-translation invariance, we have a set of r local "laws" near each point of origin. But having r in the formula (90) fixed by imposing some additional condition, or being integrated out, should *restore* the global time-translation invariance completely as long as the exponential function is considered. Moreover, stability of the exponential function is measured by the exponential function with same symmetry (see formula (92)). Not only exponential function is time-translation invariant, but the expected return β has the same property. For exponential functions the expected (predicted) value of return per unit time, exactly equals β. Note, that shifted exponential function $E_s(t,a) = c + (a-c)\exp(bt)$, with initial condition a and arbitrary b, c, is invariant under time-translation as well.

Preprints (www.preprints.org) | NOT PEER-REVIEWED | Posted: 11 September 2020 doi:10.20944/preprints202009.0141.v2

Another interesting symmetry is shape invariance [48], meaning

$$F^P_{t+\tau} = \mathsf{m} F^P_t,$$

and an exponential function is shape invariant with $\mathsf{m} = \exp(\beta\tau)$, leaving expected return unchanged. Mind that our task is to calculate β from the time series. In principle, one can think about breaking/restoration of shape invariance, as a guide for construction of the concrete scheme for calculations.

For critical phenomena an underlying symmetry of formula for observable, is scaling

$$\phi_{\lambda t} = \Lambda \phi_t,$$

where $\Lambda = \phi_\lambda$. The class of power laws, $\phi_t = t^\alpha$, with critical index α, is scaling-invariant. The central task is to calculate c. The statistical renormalization group formulated by Wilson, see. e.g. [49], explains well the critical index in equilibrium statistical systems. When information on the critical index is encoded in some perturbation expansion, one can use resummation ideas to extract the index, even for short expansions and for non-equilibrium systems [50, 3, 9]. Some of the methods were discussed in the Introduction.

Working with power-law function will not leave the return unchanged. Yet, one can envisage the scheme with broken scaling invariance, as alternative to the former schemes. The log-periodic solutions extend the simple scaling [56], and are extensively employed in the form of a sophisticated seven-parametric fit to long historical data set [43], as well as of its extensions [57]. The fit is tuned for prediction of the crossover point to a crash, understood as catastrophic downward acceleration regime [39]. But one can not exclude the possibility of the solutions with different time of symmetries (scaling and time-invariance, for instance) competing to win over, or to coexist, all measured in terms of their stability characteristics.

Our primary concern is crash per se, not the regime preceding it. We start analyzing crash with the polynomial approximation that respects time-translation symmetry, then have the symmetry broken, and then restored (completely, or partially), by means of some optimization. Such sequence ends with a non-trivial outcome: β becomes renormalized $\beta(r)$, with r to be found from optimization procedure(s) defined below.

In the paper [35], the framework for technical analysis of time series was developed based on second-degree regression and asymptotically equivalent exponential approximants, with some rudimentary, implicit breaking of the symmetry. We intend to go to higher-degree regressions and and develop

Preprints (www.preprints.org) | NOT PEER-REVIEWED | Posted: 11 September 2020 doi:10.20944/preprints202009.0141.v2

some consistent technique for explicit symmetry breaking with its subsequent restoration. According to textbooks, fourth order should be considered as "high". Taleb, see footnote on p.53 in [33], also considers models with five parameters as more than sufficient.

4.1 Optimization, approximants, multipliers

Higher-order regressions allow for replica symmetry. For instance, the quadratic regression $s_{0,2}(t) = a_2 + b_2 t + c_2 t^2$, can be replicated as follows:

$$s_{r,2}(t) = A_2(r) + B_2(r)(t-r) + C_2(r)(t-r)^2,$$

with

$$A_2(r) = a_2 + b_2 r + c_2 r^2,\ B_2(r) = b_2 + 2c_2 r,\ C_2(r) = c_2.$$

With such transformed parameters we find that $s_{r,2}(t) \equiv s_{0,2}(t)$. In fact, one can still formulate self-similarity analogous to (89), but in vector form with increased number of parameters/initial conditions in place of a [47]. But if only the linear part of quadratic regression, or trend, is taken into account, we return to the conventional functional self-similarity $\equiv$ time-translation invariance, discussed above extensively.

Such effective linear/trend approach to higher-order regressions allows to apply the same idea in all orders and observe how the exponential structures change with increasing regression order.

To take into account the dependence on origin, the replica symmetry has to be broken. Breaking of the symmetry means the dependence on origin of actual extrapolations with non-polynomial predictors. As the primary predictors we suggest the simplest exponential approximants considered as the function of origin r and time,

$$E_1^*(t,r) = A(r)\exp\left(\frac{B(r)}{A(r)}\,(t-r)\right), \tag{91}$$

independent on the order of polynomial regression. The approximants (91) are constructed by requiring an asymptotic equivalence with linear part of chosen polynomial regression. If the extrapolations $E_1^*(t_N + \delta t, r)$ are made by each of the approximants, they appear to be different for various r, meaning breaking of the replica symmetry and of the time-translation symmetry. Passage from polynomials to exponential functions leads to emergence of the continuous spectrum of relaxation (growth) times.

Preprints (www.preprints.org) | NOT PEER-REVIEWED | Posted: 11 September 2020 doi:10.20944/preprints202009.0141.v2

To compare the approximants quality, on can look at their stability. Stability of the approximants is characterized by the so-called multipliers defined as the variation derivative of the function with respect to some initial approximation function [36]. Following [58], one can take the linear regression as zero approximation, and find the multiplier

$$M_1^*(t,r) = \exp\left(\frac{B(r)}{A(r)}(t-r)\right). \tag{92}$$

The simple structure of multipliers (92) allows to avoid appearance of spurious zeroes which often complicate analysis with more complex approximants/multipliers.

Because of multiplicity of solutions, embodied in their dependence of origin, it is both natural and expedient to introduce probability for each solution. As explained in [36], one can introduce

$$Probability \propto |M_1^*(t,r)|^{-1},$$

with proper normalization, as shown below in formula (94). Probability appears to be of a pure dynamic origin and is expressed only from the time series itself. When the approximants and multipliers of the first order are applied to the starting terms of the quadratic, third or fourth order regression, we are confined to *effective first-order models*, with velocity parameter from [35] dependent also on higher order coefficients and origin.

To make extrapolation with approximants (91) one has still to know the origin. In other words, the time-translation symmetry has to be restored completely or partially, so that a specific predictor with specifically selected origin but, otherwise as close as possible to time-translation invariant form, is devised. Fixing unique origin also selects unique relaxation (growth) time during which the price is supposed to find a time-translation invariant state. Exponential functions are chosen above because they are invariant under time translation. Any shift in origins is absorbed by the pre-exponential amplitude and does not influence the return R. Similar in spirit view that broken symmetries have to be restored in a correct theory was expressed in [59].

In the approach predominantly adopted in this section, we keep the form and order of approximants the same in all orders, but let the series/regressions evolve into higher orders. Independent on the order of regression, we construct the same approximant, based only on the first order

Preprints (www.preprints.org) | NOT PEER-REVIEWED | Posted: 11 September 2020 doi:10.20944/preprints202009.0141.v2

terms, only with parameters changing with increasing order of regression. In the framework of the effective first order theories, we employ exponential approximants.

Consider the value of origin as an optimization parameter [28]. To find it and to restore the time-translation symmetry, we have to impose an additional condition directly on the exponential predictors with known last closing price,

$$E_1^*(t_N, r) = s_N\,. \tag{93}$$

One has to solve the latter equation to find the particular origin(s) $r = r^*$. In this case we consider a discrete spectrum of origins, consisting of several isolated values. To avoid double-counting when the last closing price enters both regression and optimization, one can determine the regression parameters in the segment limited from above by t_{N-1}, s_{N-1}. Or, alternatively, one can consider the two ways to define regression parameters and choose the one which leads to more stable solutions. Unless otherwise stated, we consider that such comparison was performed and the most stable way was selected.

The extrapolation for the price is simply $s(t_N+\delta t) = E_1^*(t_N+\delta t, r^*)$. The condition imposed by the equation (93) is natural, because then, a first-order approximation to the formula (88), $R \approx \frac{s(t_N+\delta t)-s(t_N)}{s(t_N)}$, is recovered (see, e.g., [38]), as one would expect intuitively.

The procedure embodied in (93), leads to a radical reduction of the set of r-predictors to just a few. Set of predictors and corresponding to each multiplier, define the probabilistic, poor man's order book. Instead of an unknown to us true numbers of buy and sell orders, we calculate a priori probabilities for the price going up or down and corresponding levels. Target price is estimated through weighted averaging developed in [36, 58], in its concrete form (94) given below.

For sake of uniqueness one can simply choose the most stable result among such conditioned predictors. One can also consider extrapolation with weighted average of all such selected solutions. With $1 \leq M \leq 6$ solutions, their weighted average $\overline{E}_1$ for the time $t_N + \delta t$ is given as follows,

$$\overline{E}_1(t_N + \delta t) = \frac{\sum_{k=1}^{M} E_1^*(t_N + \delta t, r_k^*)\,|M_1^*(t_N + \delta t, r_k^*)|^{-1}}{\sum_{k=1}^{M} |M_1^*(t_N + \delta t, r_k^*)|^{-1}}. \tag{94}$$

Within the discrete spectrum we can find solutions with varying degree of adherence to the original data. They can follow data rather closely or be loosely defined by the parameters of regression. The former could be called

Preprints (www.preprints.org) | NOT PEER-REVIEWED | Posted: 11 September 2020 doi:10.20944/preprints202009.0141.v2

"normal" solutions, and tend to be less stable, with multipliers ~ 1, but the latter are "anomalous" solutions, since they cut through the data, and typically are the most stable with small multipliers. Anomalous solutions are crashes (meltdowns), and melt-ups. Typical situation with the solutions in the discrete spectrum is presented in Fig.10. The novel feature introduced through (94), is that averaging is performed over all approximants of the same order, compatible with constraints expressed by (93).

One can also integrate out the dependence on origin r, considered as continuous variable, by applying an averaging technique of weighted fixed points suggested in [36]. The dependence on origin enters the integration limit through parameter T. Integration can be performed numerically for the simplest exponential predictors according to the formula

$$I(t,T) = \frac{\int_{t_0-T}^{t_N+T} E_1^*(X,t)\,|M_1^*(X,t)|^{-1}\,dX}{\int_{t_0-T}^{t_N+T} |M_1^*(X,t)|^{-1}\,dX}. \tag{95}$$

To optimize the integral we have to impose an additional condition on the weighted average/integral. It is natural to force it pass precisely through the last historical point.

$$I(t_N,T) = s(t_N), \tag{96}$$

and solve the latter to find the integration limit $T = T^*$. The sought extrapolation value for the price s is simply $I(t_N + \delta t, T^*)$.

As an additional condition to find origin, one can also consider the minimal difference requirement on the lowest order predictors, as first suggested in [40]. To this end one has to construct the second order super-exponential approximant

$$\begin{aligned} E_2^*(t,r) &= A(r)\exp\left(\frac{B(r)(t-r)\exp\left(\frac{C(r)(t-r)\tau(r)}{B(r)}\right)}{A(r)}\right), \\ \tau(r) &= 1 - \frac{B(r)^2}{2A(r)C(r)}, \end{aligned} \tag{97}$$

and minimize its difference with the simplest exponential approximant in the time of interest $t_N + \delta t$. Namely, one has to find all roots of the equation

$$\exp\left(\frac{C(r)\tau(r)(t_N+\delta t-r)}{B(r)}\right) = 1, \tag{98}$$

with respect to real variable r. Corresponding multiplier

$$M_2^*(t,r) = \frac{1}{B(r)}\frac{\partial E_2^*(t,r)}{\partial t},$$

Preprints (www.preprints.org) | NOT PEER-REVIEWED | Posted: 11 September 2020 doi:10.20944/preprints202009.0141.v2

can be found as well.

The discrete spectrum optimization seems to be the most natural and transparent. Our goal is to find the approximants and probabilistic distributions in the last available historical point of time series. Crashes are attributed to the stable solutions with large negative r, meaning that origin of time has to be moved to the deep past to explain crash in near future. Preliminary results of [28], suggest that in overwhelming majority of cases, crash is preceded by similar, asymmetric probability pattern(s), of the type shown in figures below [1]. There are also additional solutions with multipliers of the order of unity, coming form with the region of moderate r, and it is often possible to find some rather stable upward solution for large positive r. One can think that for such stable time series as describing population dynamics, the region of moderate r gives relevant solutions, while for time series describing price dynamics all types of solutions exist simultaneously.

Within our approach to constructing approximants one can also try to exploit the second order terms in regression. Instead of exponential approximants one should try some other, higher order approximants, but with time-translation invariance property. Such approximants are presented below. They are considered *ad hoc*, because they can be written in closed from only in special, low-order situations. It is not feasible to extend them systematically into arbitrary high order, in contrast with approximants mentioned in the context of first approach. On the contrary, all approximants mentioned for the first approach, violate the time-translation invariance, and can not be used purpose of symmetry restoration. Hence, our interest in special forms with desired symmetry. But all three approaches could be applied simultaneously and complementary, since the price evolution can take various unexpected forms. Sometimes, it is even not possible to find stable solutions with third approach, but is possible with corrected approximants.

Recall that exponential function can be obtained as the solution to simple linear first order ODE. In search of second order approximants with time-translation invariance, we turned to some explicit formulas, emerging in the course of solving some first order ODE with added nonlinear term with arbitrary positive power, which generalizes ODE for simple exponential growth. It is known as Bertalanffy-Richards(BR) growth model [60, 61]. Among its solutions in the case of second-order nonlinear term, there is a celebrated lo-

[1] As noted in [41], Kahneman and Tversky explained that people tend to judge current events by their similarity to memories of representative events.

Preprints (www.preprints.org) | NOT PEER-REVIEWED | Posted: 11 September 2020 doi:10.20944/preprints202009.0141.v2

gistic function [60], $L(t) = \frac{1}{q_2 + \frac{(1-q_1 q_2)\exp(-q_0 t)}{q_1}}$, where q_1 is the initial condition. The logistic function is widely used to describe population growth phenomena and is also known to be the solution to logistic equation of growth. The logistic function written in the form $L(t, q_1)$, dependent on the initial condition $L(0, q_1) = q_1$, with arbitrary q_0, q_2, is time-translation invariant. One can also introduce the second-order logistic approximant which generalizes logistic function [28]. In addition to describing situations with saturation at infinity, the logistic approximant include also the case of so-called finite-time singularity, which makes it redundant, since such solutions were excluded from the price dynamics [35].

Another solution to the Bertalanffy-Richards model in the case when the nonlinear term has power only slightly differing from unity, is known as Gompertz function [60],

$$G(t) = g_0 \exp(g_1 \exp(g_2 t)), \tag{99}$$

used to describe growth (relaxation, decay) phenomena. But, as we demonstrate in the very end of Introduction, it is possible to explain $G(t)$ directly from the resummation technique leading to the formula (19), without resorting to BR. Relaxation time(growth) behaves exponentially with time. Gompertz function is *log*-time-translation invariant.

One can consider the second order Gompertz approximant. It simply generalizes the Gompertz function. Namely, one can find Gompertz approximant in the following form

$$\begin{aligned} &G(t, r) = g_0(r) \exp(g_1(r) \exp(g_2(r)(t - r))), \\ &g_0(r) = A(r) e^{-g_1(r)}, \quad g_1(r) = \frac{B(r)}{A(r) g_2(r)}, \quad g_2(r) = \frac{2A(r)C(r) - B(r)^2}{A(r)B(r)}, \end{aligned} \tag{100}$$

with the multiplier

$$M_G(t, r) = \frac{g_0(r) g_1(r) g_2(r) e^{(g_1(r) e^{g_2(r)(t-r)} + g_2(r)(t-r))}}{B(r)}.$$

The Gompertz approximant, of course, is not limited to the situations with saturation at infinity, as it can describe also very fast decay (growth) at infinity.

With r to be found from some optimization procedure, the return R generated by Gompertz approximant, is time-translation invariant, and has a compact form

$$R(\delta t) = g_1(r) \exp(g_2(r)(t_N - r))(\exp(g_2(r)\delta t) - 1).$$

Preprints (www.preprints.org) | NOT PEER-REVIEWED | Posted: 11 September 2020 doi:10.20944/preprints202009.0141.v2

For small δt it becomes particularly transparent:

$$R(\delta t) \approx g_1(r)g_2(r)\exp(g_2(r)(t_N - r)) \times \delta t \equiv \frac{\delta t}{\tau(T_N, r)},$$

with the pre-factor giving the return per unit time. The inverse return per unit time has the physical meaning of the effective time for growth (relaxation)

$$\beta(t,r)^{-1} \equiv \tau(t,r) = (g_1(r)g_2(r))^{-1}\exp\left(g_2(r)(r-t)\right),$$

considered at the moment $t = T_N$. Here, we employed the the effective relaxation (growth) time (see Introduction), $\tau(t) = \left(\frac{d}{dt}\ln G(t)\right)^{-1}$, and replicated it. We can find the return for Gompertz approximant solely determined by relaxation

$$\mathbf{S}(t,r) = \frac{1}{\tau(t,r)},$$

and express the log return in a compact form

$$R(\delta t) = \mathbf{S}(t_N + \delta t, r) - \mathbf{S}(t_N, r).$$

Thus, the return for Gompertz approximant is purely dynamic quantity. If relaxation time is found from the data to be very large as it should be close to equilibrium conditions [62], we have no potential for returns, i.e., near-equilibrium yields dull, everyday mundane events that are repetitive and lend themselves to statistical generalizations [39]. If relaxation time is anticipated to be very short, we have potentially huge returns, and conclude that far-from-equilibrium conditions give rise to unique, historic events [39].

Gompertz approximant can go at infinity faster or slower than exponential, and in some important examples such difference amounting to a few percents, can be detected. The function $g_0(r)$, could be called a gauge function for the price, expressing arbitrariness of choice of the price unit, as it does not enter the return. The time-translation invariance of return and gauge invariance for the price are considered very desirable in price model formulation [35], both properties are pertinent to exponential and Gompertz approximations for the price temporal dynamics.

We are interested in market prices on a daily level, and consider only significant market price drops/crashes with magnitude more than 5.5%. Such magnitude is selected to be comparable to the typical yearly return of Dow Jones Industrial Average index. Typically, a 2% daily move is considered

Preprints (www.preprints.org) | NOT PEER-REVIEWED | Posted: 11 September 2020 doi:10.20944/preprints202009.0141.v2

as big, but not at the times of various turmoils. It is widely accepted in practical finance that asset price moves in response to unexpected fundamental information. The information can be identified as well as the tone, positive versus negative. It is found that news arrival is concentrated among days with large return movements, positive or negative [64]. Spontaneously emerging narratives, a simple story or easily expressed explanation of events, might be considered as largely exogenous shocks to the aggregate economy [41]. Simply put, one should analyze what people are talking about in search for the source of economic fluctuations. Moreover, just like in true epidemics governed by evolutionary biology, mutations in narratives spring up randomly, just as in organisms in evolutionary biology, and if contagious generate unpredictable changes in the economy [41]. As noted in [65], panic on the market can be due to external shocks or self-generated nervousness. It is argued [66], that cause and effect can be cleanly disentangled only in the case of exogenous shocks, as it is only needed to select some interesting set of shocks to which price is likely to respond. Effects of positive and negative oil price shocks on the stock price need not be symmetric. In macroeconomics it is even accepted that only positive changes in the price of oil have important effects. Periods dominated by oil price shocks are reasonably easy to identify, and they can be indeed considered as exogenous and, often, strong, although difficult to model. Oil price shocks are the leading alternative to monetary shocks, and may very well have similar effects [66].

4.2 Example

Consider as example a 7.72% drop in the value of Shanghai Composite index related to the first COVID-19 crash, which occur on February 3, 2020. With $N = 15$, as recommended in [35], the following data points available,

$$s_0 = 3085.2, s_1 = 3083.79, s_2 = 3083.41, s_3 = 3104.8, s_4 = 3066.89, s_5 = 3094.88,$$

$$s_6 = 3092.29, s_7 = 3115.57, s_8 = 3106.82, s_9 = 3090.04, s_{10} = 3074.08, s_{11} = 3075.5,$$

$$s_{12} = 3095.79,\ s_{13} = 3052.14,\ s_{14} = 3060.75,\ s_{15} = 2976.53.$$

And the value of $s_{16} = 2746.61$ is to be "predicted". From the whole set of daily data we employ only several values of the closing price. Such coarse-grained description of the time series may be justified if one is interested in the phenomenon not dependent on the fine details, such as crash. In the

Preprints (www.preprints.org) | NOT PEER-REVIEWED | Posted: 11 September 2020 doi:10.20944/preprints202009.0141.v2

examples presented below, we keep the number of data points per quartic regression parameter in the range from 3 to 4. Lower order calculations can be found in [28]. Here we show only the quartic regression

$$s_{0,4}(t) = a_4 + b_4 t + c_4 t^2 + d_4 t^3 + f_4 t^4,$$

and based on it optimized approximants and multipliers. It can be replicated as follows:

$$s_{r,4}(t) = A_4(r) + B_4(r)(t-r) + C_4(r)(t-r)^2 + D_4(r)(t-r)^3 + F_4(r)(t-r)^4,$$

with

$$A_4(r) = a_4 + b_4 r + c_4 r^2 + d_4 r^3 + f_4 r^4,\ B_4(r) = b_4 + 2c_4 r + 3d_4 r^2 + 4f_4 r^3,$$

$$C_4(r) = c_4 + 3d_4 r + 6f_4 r^2, \quad D_4(r) = d_4 + 4f_4 r, \quad F_4(r) = f_4.$$

With such transformed parameters we have $s_{r,4}(t) \equiv s_{0,4}(t)$.

Within the data shown in Fig.8, one can discern competing trends. First, let us show the data compared to the regression. There are two obvious trends, "up" and "down" as can be seen in Fig.8. Our analysis will indeed

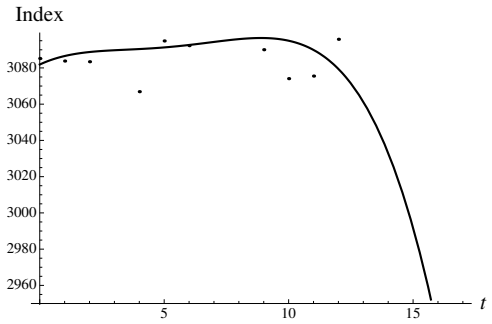

Figure 8: COVID-19, Shanghai Composite, February 3, 2020. Fourth-order regression against data points

find highly probable solutions of both types, with the downward trend developing into fast exponential decay. Let us analyze the typical approximant and multiplier dependencies on origin, for fixed time $t = t_N$. The inverse multiplier is shown as function of the origin r in Fig.9 as well as the first order approximant. There are two uneven humps in the probabilistic inverse

Preprints (www.preprints.org) | NOT PEER-REVIEWED | Posted: 11 September 2020 doi:10.20944/preprints202009.0141.v2

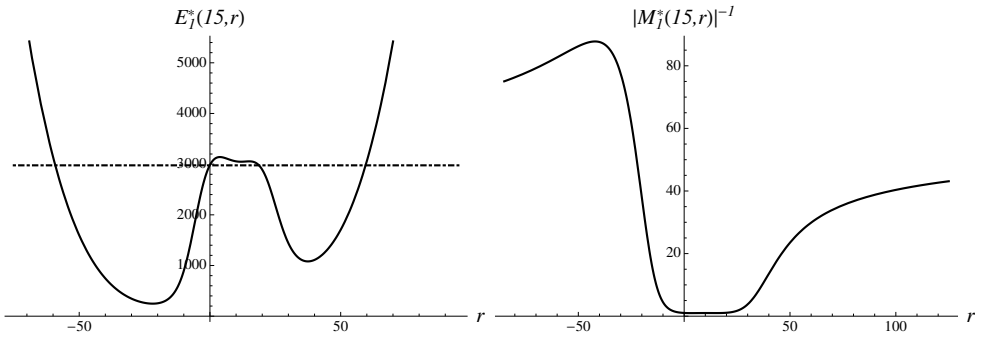

Figure 9: Shanghai Composite, February 3, 2020. Calculations with fourth-order regression. The inverse multiplier is shown as function of the origin r at $t = T_N$, $N = 15$. The first order approximant is shown at separate figure. Level s_{15} is shown as well, with dot-dashed line.

multiplier, suggesting that large negative and large positive r dominate, with more weight put on the negative region. Such dependence on r manifests the time-translation invariance violation, which should be lifted by finding appropriate origin. More details on the example can be found in [28]. Below we discuss only the fourth-order calculations.

The results of extrapolation by method expressed by equation (93) is given as

$$E_1^*(16) = 2804.32, \quad M_1^*(16) = 0.0113494,$$

with relative percentage error of 2.1%. There is also less stable "upward" solution

$$E_1^*(16) = 3211.95, \quad M_1^*(16) = 0.0363796,$$

in agreement with intuitive picture based on naive data analysis. There are also two additional solutions in between with multipliers close to 1. They do not effect averages much, but in real time the metastable solutions, just like metastable phases in condensed matter, may show up under special conditions. Metastable solutions when realized, violate principle of maximal stability over the observation timescale, complicating or even negating a unique forecast, based on weighted averages or the most stable solution.

Calculation of the discrete spectrum can be extended to different approximants. For instance, one can also construct the second order Gompertz

Preprints (www.preprints.org) | NOT PEER-REVIEWED | Posted: 11 September 2020 doi:10.20944/preprints202009.0141.v2

approximant introduced above, and solve the following equation on origins,

$$G(t_N, r) = s(t_N)\,. \tag{101}$$

The most stable Gompertz approximant gives the most accurate estimate

$$G(16) = 2746.05, \quad M_G(16) = 0.001539,$$

with very small error of 0.02%. There are altogether five solutions to (101), in the discrete spectrum as shown in Fig.10. Thus, the Gompertz approximant

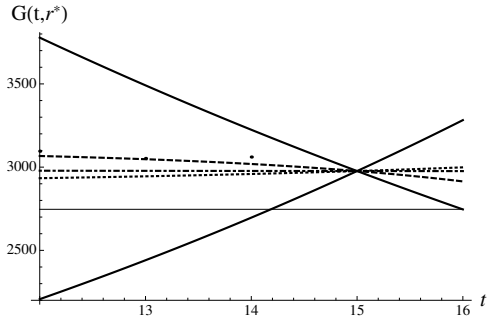

Figure 10: All Gompertz approximants corresponding to the discrete spectrum, i.e., solutions to (101) are shown. The most stable downward and less stable upward solutions are shown with solid lines. Three additional solutions are shown as well. The solution shown with dashed line is closest to the data. The "no-change", practically flat solution, is shown with dot-dashed line. Yet another solution, corresponding to moderate growth, is shown with dotted line. The level $s_{16} = 2746.61$ is shown with black line. Several historical data points are shown as well.

of second order with log-time-translation invariance, gives better results than symmetric exponential approximant E_1^*. Although Taleb's Black Swan did seem to materialize, the short-time stock market response was not different than in somewhat comparable instances of crashes brought up in [28], making it look like a Grey Swan. Indeed, it is plausible that a holiday season in China, played the role here. It also helped our cause, effectively pinpointing the day for crash. One can think that all solutions, except the most extreme downward solution, where simply not considered.

Preprints (www.preprints.org) | NOT PEER-REVIEWED | Posted: 11 September 2020 doi:10.20944/preprints202009.0141.v2

4.3 Comments

Many more examples of various notable crashes can be found in [28]. They were selected to exemplify market reaction to shock including 9/11, Fukushima disaster, US entrance to the Great War, death of Chinese leader Deng Xiaoping, Friday the 13th, flash crash etc.,and to demonstrate similarity of early panics with coronavirus recession. Despite their different "geometry", different temporal patterns preceding crash, exhibit analogous in their main features probabilistic distributions, with significant difference only in the region of moderate r, but with analogous structure for large negative and positive origins. Crashes are attributed to the stable solutions with large negative r, meaning that origin of time has to be moved to the deep past to explain crash in near future. Preliminary results of [28], suggest that in overwhelming majority of cases, crash is preceded by similar, asymmetric probability pattern(s), of the type shown in figures of this section.

Exponential and Gompertz approximants are found to work rather well, despite(or due to?) their simplicity. Unlike all other approximants they give very clear graphic snapshot of the probabilistic space. Besides, their application is grounded in the exponential form of any future contract, with a transparent interpretation to the renormalized trend parameter $\beta(t, r)$, as expected return per unit time, equivalent to as inverse growth (relaxation) time.

Our theory explains or at least give a hint why making predictions about the future is so notoriously difficult. Instead of a unique, ironclad solution to the problem we advocate finding all solutions and interpret them as bounds as plainly illustrated in Fig.10. Bounds are given different strength, a priori determined by multipliers. Reality is not completely confined to reaching the most stable bound, but various metastable bounds can be realized as well, blurring the picture and complicating emergent time dynamics.

After applying some arguments concerned with broken/restored time-invariance, we come to the exponential solution with explicit finite time scale, which was only implicit in initial parametrization with polynomial regressions. Mind that in condensed matter physics and field theory there is a key Meissner-Higgs mechanism for generating mass or, equivalently, for creating some typical space scale from original fields through broken symmetry technique (see, e.g.,[63]). Relatively recently the concept was confirmed, culminating in discovery of the Higgs boson. Our approach to market price evolution is by all means inspired by Meissner-Higgs effect. But, instead of a

Preprints (www.preprints.org) | NOT PEER-REVIEWED | Posted: 11 September 2020 doi:10.20944/preprints202009.0141.v2

mass of mind-boggling elementary particle, we have a mundane, but highly sought after return per unit time.

References

[1] G.A.Baker, P. Graves-Moris, Padé approximants, Cambridge, UK: Cambridge University; 1996.

[2] S. Gluzman, V.I. Yukalov, Self-similarly corrected Pad'e approximants for indeterminate problem, European Physical Journal Plus, 131, 340-361, 2016.

[3] S. Gluzman, V. Mityushev, W. Nawalaniec, Computational analysis of structured Media, Academic Press (Elsevier), 2017.

[4] I. Andrianov, J. Awrejcewicz, V. Danishevs'kyy, S. Ivankov, Asymptotic methods in the theory of plates with mixed boundary conditions, John Wiley & Sons, 2014.

[5] S. Gluzman, V.I. Yukalov, Effective summation and interpolation of series by self-similar approximants, Mathematics, 3, 510–526, 2015.

[6] S. Gluzman, V.I. Yukalov, D. Sornette, Self-similar factor approximants. Phys. Rev. E, 67, 026109, 2003.

[7] V. Yukalov, S. Gluzman, Self-similar exponential approximants, Phys. Rev. E. 58, 1359–1382, 1998.

[8] L.A. Gavrilov, N.S. Gavrilova, The reliability theory of aging and longevity, J.Theor.Biol.213, 527-453, 2001.

[9] P. Dryga' s, S. Gluzman V. Mityushev, W. Nawalaniec, Applied analysis of composite media, Woodhead Publishing (Elsevier), 2020.

[10] S. Torquato, Random heterogeneous materials: Microstructure and macroscopic properties, New York,Springer-Verlag: 2002.

[11] P.M. Adler, Porous media. Geometry and transport, edition 2nd, New York, Butterworth-Heinemann; 1992.

Preprints (www.preprints.org) | NOT PEER-REVIEWED | Posted: 11 September 2020 doi:10.20944/preprints202009.0141.v2

[12] P.M. Adler, A.E. Malevich, V.V. Mityushev, Nonlinear correction to Darcy's law for channels with wavy walls, Acta Mech., 224, 2013. 1823–1848.

[13] A.E. Malevich, V.V. Mityushev, P.M. Adler, Stokes flow through a channel with wavy walls, Acta Mech.,182, 151–182, 2006.

[14] K.M. Golden, S.F. Ackley, V.I. Lytle, The percolation phase transition in sea ice,Science, 282, 2238–2241, 1998.

[15] K.M. Golden, Climate change and the mathematics of transport in sea ice, Science,56, 562–584, 2009.

[16] M. J. Wolovick, J.C. Moore, Stopping the flood: could we use targeted geoengineering to mitigate sea level rise?, The Cryosphere, 12, 2955–2967, 2018.

[17] C. Pozrikidis, Creeping flow in two-dimensional channel, J. Fluid Mech.,180, 495–514, 1987.

[18] R. Wojnar, W. Bielski, Laminar flow past the bottom with obstacles – a suspension approximation. Bull. Pol. Acad. Sci., Tech. Sci. 63, 685–695, 2015.

[19] R. Wojnar, W. Bielski. Gravity driven flow past the bottom with small waviness. In: Drygas, P., Rogosin, S. (Eds.), Modern Problems in Applied Analysis. In: Trends in Mathematics. Birkhauser,181–202, 2018.

[20] W. Bielski, R. Wojnar. Stokes flow through a tube with wavy wall. In: Awrejcewicz, J. (Ed.), Dynamical Systems in Theoretical Perspective. DSTA 2017. In: Springer Proceedings in Mathematics & Statistics. Springer, Cham,379–390, 2018.

[21] M.Rasoulzadeh, M.Panfilov, Asymptotic solution to the viscous/inertial flow in wavy channels with permeable walls. Phys. Fluids 30, 106604. 2018.

[22] R. Czapla, V. Mityushev, W. Nawalaniec. Macroscopic conductivity of curvilinear channels. In: Jaworska, L. (Ed.), Int. Conf. Engineering, Education and Computer Science. Pedagogical University, Krakow, 2010.

Preprints (www.preprints.org) | NOT PEER-REVIEWED | Posted: 11 September 2020 doi:10.20944/preprints202009.0141.v2

[23] V. Mityushev, N. Rylko. Mathematical model of electrokinetic phenomena in two-dimensional channels. In: Jaworska, L. (Ed.), Int. Conf. Engineering, Education and Computer Science. Pedagogical University, Krakow, 5–20, 2010.

[24] P.M. Adler, J. Thovert, Fractures and Fracture Networks, edition 2nd, New York: Kluwer,1999.

[25] M. Scholle, Creeping Couette flow over an undulated plate, Arch. Appl. Mech.,73, 823–840, 2004.

[26] H. K. Moffatt, Viscous and resisitive eddies near a sharp corner, J.Fluid. Mech.,18, 1–18, 1964. See also H. K. Moffat: Corner flow : a classical problem with a new twist.: http://docslide.us/documents/hk-moffatt-corner-flow-a-classical-problem-with-a-new-twist.html

[27] S. Gluzman, V. Yukalov, Unified approach to crossover phenomena, Phys. Rev. E 58, 4197-4209, 1998.

[28] S. Gluzman, Market crashes and time-translation invariance. Quantitative technical analysis, DOI: 10.13140/RG.2.2.22623.07842/1, June 2020.

[29] K. Brading, E. Castellani, N. Teh, Symmetry and symmetry breaking, The Stanford Encyclopedia of Philosophy (Winter 2017 Edition), Edward N. Zalta (ed.).

[30] O. Peters. Optimal leverage from non-ergodicity, Quant. Fin., 11, 593–1602, 2011.

[31] O. Peters, W. Klein, Ergodicity breaking in geometric Brownian motion, Phys. Rev. Lett., 110, 100603, 2013.

[32] O. Peters, M. Gell-Mann, Evaluating gambles using dynamics, Chaos. 26(2):023103, 2016.

[33] N. N. Taleb, Statistical Consequences of Fat Tails (Technical Incerto Collection), 2020.

[34] K. Sacha, Modeling spontaneous breaking of time-translation symmetry, Phys. Rev. A 91, 033617, 2015.

Preprints (www.preprints.org) | NOT PEER-REVIEWED | Posted: 11 September 2020 doi:10.20944/preprints202009.0141.v2

[35] J. V. Andersen, S. Gluzman, D. Sornette, General framework for technical analysis of market prices, Europhys. J. B 14, 579–601, 2000.

[36] V.I. Yukalov, S. Gluzman, Weighted fixed points in self-similar analysis of time series, Int. J. Mod. Phys. B 13, 1463–1476, 1999.

[37] A. Mann, Market forecasts, Nature 538, 308–310, 2017.

[38] M. Fliess, C. Join, A mathematical proof of the existence of trends in financial time series, arXiv: 0901.1945v1 [q-fin.ST] 14 Jan 2009.

[39] G. Soros, Fallibility, reflexivity, and the human uncertainty principle, Journal of Economic Methodology, 20, 309-329, 2013.

[40] S. Gluzman, V. Yukalov, Renormalization group analysis of October market crashes, Mod. Phys. Lett. B 12, 75–84, 1998.

[41] R.J. Shiller, Narrative economics, American Economic Review 107, 967–1004, 2017.

[42] V. I. Arnold, Mathematical methods of classical mechanics, Springer-Verlag, 1989.

[43] Q. Zhang, Q. Zhang, D. Sornette, Early warning signals of financial crises with multi-scale quantile regressions of log-periodic power law singularities. PLoS ONE 11, e0165819, 2016.

[44] S. Gluzman, V. Yukalov, Booms and crashes of self-similar markets, Mod. Phys. Lett. B 12, 575–587, 1998.

[45] N. N. Bogoliubov, D. V. Shirkov, Quantum fields. Benjamin-Cummings Pub. Co., 1982.

[46] D.V. Shirkov, The renormalization group, the invariance principle, and functional self-similarity, Sov. Phys. Dokl. 27, 197–199, 1982.

[47] H. Kröger, Fractal geometry in quantum mechanics, field theory and spin systems, Phys. Rep. 323, 81–181, 2000.

[48] J. Bougie, A. Gangopadhyaya, J. Mallow, C. Rasinariu, Supersymmetric quantum mechanics and solvable models, Symmetry 4, 452–473; doi:10.3390/sym4030452, 2012.

Preprints (www.preprints.org) | NOT PEER-REVIEWED | Posted: 11 September 2020 doi:10.20944/preprints202009.0141.v2

[49] S. Ma, Theory of critical phenomena, Benjamin, London, 1976.

[50] S. Gluzman, V.I. Yukalov, Critical indices from self-similar root approximants, The European Physical Journal Plus 132: 535, 2017.

[51] S. Gluzman, V. I. Yukalov, Self-Similar Power Transforms in Extrapolation Problems, J. Math. Chem. 39, 47–56, 2006.

[52] V. I. Yukalov, S. Gluzman, Optimization of Self-Similar Factor Approximants, Molecular Physics, 107, 2237–2244, 2009.

[53] V. I. Yukalov, Statistical mechanics of strongly nonideal systems, Phys. Rev. A 42, 3324–3334, 1990.

[54] V. I. Yukalov, Method of self-similar approximations, J. Math. Phys., 32, 1235–1239, 1991.

[55] V.I. Yukalov, Stability conditions for method of self-similar approximations, J. Math. Phys., 33, 3994–4001, 1992.

[56] S. Gluzman, D. Sornette, Log-periodic route to fractal functions, art. no. 036142. Physical Review E, V6503 N3 PT2A:U418-U436, 2002.

[57] C. Lynch, B. Mestel, Logistic model for stock market bubbles and anti-bubbles, International Journal of Theoretical and Applied Finance, 20(6), article no. 1750038, 2017.

[58] V.I. Yukalov, S. Gluzman, Extrapolation of power series by self-similar factor and root approximants, Int. J. Mod. Phys. B 18, 3027–3046, 2004.

[59] T. Duguet, J. Sadoudi, Breaking and restoring symmetries within the nuclear energy density functional method, J.Phys.G: Nucl. Part. Phys. 37, 064009, 2010.

[60] Y.C. Lei, S.Y. Zhang, Features and partial derivatives of Bertalanffy-Richards growth model in forestry, Nonlinear Analysis: Modelling and Control, 9, 65–73, 2004.

[61] F. J. Richards, A flexible growth function for empirical use, J. Exp Bot., 10, 290–301, 1959.

Preprints (www.preprints.org) | NOT PEER-REVIEWED | Posted: 11 September 2020 doi:10.20944/preprints202009.0141.v2

[62] S. Gluzman, D. Karpeev, Perturbative expansions and critical phenomena in random structured media, In Book "Modern Problems in Applied Analysis", Eds. P. Drygaś and S. Rogosin, 117–134, Birkhauser, 2017.

[63] H. Kleinert, Vortex origin of tricritical point in Ginzburg–Landau theory, Europhys. Lett., 74, 889–895, 2006.

[64] J. Boudoukh, R. Feldman, S. Kogan, M. Richardson, Which news moves stock prices? A textual analysis, NBER Working Paper No. 18725 January 2012,

[65] D. Harmon, M. Lagi, M. A. M. de Aguiar, D. D. Chinellato, D. Braha, I. R. Epstein, Y. Bar-Yam, Anticipating economic market crises using measures of collective panic, PLoS ONE 10(7): e0131871. doi:10.1371/journal.pone.0131871, 2015.

[66] B. S. Bernanke, M. Gertler, M. Watson, Systematic monetary policy and the effects of oil price shocks, Brookings Papers on Economic Activity, 1, 91–157, 1997.